STUK-YTO-TR 193 / OCTOBER 2002

OIL POOL FIRE IN A LARGE TURBINE HALL

CFD simulation

Risto Huhtanen

(VTT Processes)

In STUK this study was supervised by Jouko Marttila

STUK • **SÄTEILYTURVAKESKUS**
STRÅLSÄKERHETSCENTRALEN
RADIATION AND NUCLEAR SAFETY AUTHORITY

Osoite/Address • Laippatie 4, 00880 Helsinki
Postiosoite / Postal address • PL / P.O.Box 14, FIN-00881 Helsinki, FINLAND
Puh./Tel. (09) 759 881, +358 9 759 881 • Fax (09) 759 88 500, +358 9 759 88 500 • www.stuk.fi

ISBN 951-712-598-4 (print)
ISBN 951-712-599-2 (pdf)
ISSN 0785-9325

Dark Oy, Vantaa/Finland 2002

HUHTANEN Risto (VTT Processes). Oil pool fire in a large turbine hall—CFD simulation. STUK-YTO-TR 193. Helsinki 2002. 38 pp.

Keywords: turbine hall, oil fire, fire simulation

Abstract

In this simulation the main interest is in the general flow behaviour in the large turbine hall in a case of an oil pool fire. The fuel release rate is given in advance. In the large and rather complex geometry of the hall the main obstacles and decks that limit fluid flow are taken into account. The turbine hall is common to the two units of the power plant and includes four turbines altogether. Special attention is paid to the fire source and plume area with main deck openings by refining the grid locally at these locations. The main dimensions of the hall are length 180 m, width 42 m and height 33.1 m. The total number of fluid cells is 216 375.

Oil leak takes place under the turbine 2 on unit 1 where oil is ignited immediately and it flows down from the level of main deck to the lowest level on the side of the heat exchanger. Oil forms a pool on the floor and on one cable tunnel. The applied maximum fuel release rate corresponds about 150 MW burning rate. The heat load to the adjacent tunnels with redundant cable routes and to the sidewall of the turbine hall is calculated. Electronic devices behind the uninsulated sidewall may be damaged due to the heat load.

In the simulation it is assumed that the ventilation operates at nominal rate. The fire supression systems of the tubine hall are not taken into account in this simulation. Under these conditions the heat load to the adjacent tunnels seems not to be very high. The maximum incident radiation flux is about 5 kW/m^2 and gas temperature above the tunnels is 250–300°C. The sidewall experiences more severe heat load. The maximum radiation flux under the level +3.00 is 32–43 kW/m^2 and near the main deck 24–30 kW/m^2 at times 10–20 minutes from ignition. The maximum gas temperature under level +3.00 is 630–690°C and near the main deck 430–450°C during the same time interval.

The temperature under the ceiling reaches the level of 220°C within 20 minutes in the case where the smoke hatches are open and remove part of the heat. This temperature alone is not considered too high to affect the material strength. After 20 minutes the temperature under the ceiling is still rising.

Contents

1 Introduction

Oil pool fire on the floor of a large turbine hall is considered as a remarkable threat to the structures of the hall and possibly to some safety related equipment. In the turbine hall of Loviisa nuclear power plant there exist 56 m^3 of lubricating oil for each turbine unit. Gravity oil tanks ($2 \cdot 8.5$ m^3) and lift oil pumps ensure lubrication of the turbine-generator bearings after turbine trip. Therefore, in the case of oil leak, it is possible that even large oil pools are formed on different floors being fed by lubrication system. If the oil is ignited, the long–term fire may result in high temperature exposure to fire barriers and under the ceiling jeopardizing supporting structures of the building, as well as availability of components in the adjacent rooms.

The aim of this simulation is to find out the temporal development of the flow and temperature field in an oil pool fire. The oil pool is assumed to form and ignite under the high pressure turbine number two on unit 1 of the power plant. In this power plant layout units 1 and 2 a have a common turbine hall with four turbines altogether. The interest is also to find out how heat is transferred across the hall from unit 1 side to the unit 2 side.

On the roof there are 32 smoke hatches, which in the case of fire remove smoke and heat from the hall. The aim is to find out how large is the high temperature area under the ceiling and how much heat is extracted through the smoke hatches.

2 The hall and the structures

The length of the hall is 180 m, width 42 m and height 33.1 m with total volume of about 250.000 m^3 as calculated from the main dimensions. The turbine hall is common to the two units of the power plant and includes four turbines altogether. The computational area covers essentially the whole building. Only parts below the level +3.00 m on unit 2 side and seawater pipeline tunnel below the floor –0.60 m on unit 1 side are omitted. Part of the hall has been simulated earlier with PHOENICS code [1]. In that early simulation, symmetry assumption and simplified geometry description were used because the computational work was heavy for the computers of late 80's. This simulation is more detailed in describing the geometry and heat transfer.

Ventilation flow rate in the hall is nominally $2 \cdot 92$ m^3/s. With this rate the air content is changed almost three times in an hour. When the planned simulation time is about 20 minutes, the ventilation flow rate has to be taken into account.

There are several heat sources during the normal operation in the turbine hall. The normal heat release rate from the hot surfaces and equipment is estimated to be $2 \cdot 1000$ kW. This heat release is distributed on the turbines (50%), on main feed water pumps (20%) and other areas below the main deck +12.60m. In the first phase the normal flow and temperature conditions are calculated in a steady state simulation.

In normal conditions, fresh air is blown to the hall from air inlets on the main deck (+12.60 m) and on the lower levels. All air is extracted out from the ceiling (except that escaping through the small leaks). The fire suppression systems of the turbine hall are not taken into account in this simulation.

The structures below the main deck (+12.60 m) are mainly of concrete. The walls above the main deck and the ceiling are made of thin metal sheet with thermal insulation. The heat capacity of this is very low. The concrete structures are considered as constant temperature structures (surface temperature of 20–25°C is assumed). The insulated walls and the ceiling are modelled as adiabatic surfaces.

3 Grid and boundary conditions

3.1 Computational grid

The computational grid of the hall is defined in several parts. These are volumes below the main deck on unit 1 and unit 2 side, volumes above the main deck on unit 1 and 2 side (4 volumes), the smoke hatches on the roof (32 volumes) which makes 36 volumes altogether. The smoke hatches are equal, so one prototype is copied to 32 places on the roof. The volumes are 'glued' together with the auxiliary code *tfilter* to form a continuous computational grid. The interfaces between the parts are generally non-conformal, i.e. the number and distribution of the cells is not equal across the interface. This technique brings some freedom to the grid generation and makes it possible to have a higher resolution in the areas where needed. On the other hand, particularly in Fluent code, in this kind of grid including non-conformal interfaces, it is not possible to add new faces by separating large face to two or more sub-faces in order to introduce new boundary condition areas. If the boundary condition areas are to be changed the whole assembly of grid parts has to be done again. This is so tedious that it is not possible in practice. This has to be considered a limitation of the Fluent code.

The computational grid is unstructured, i.e. the number of cells on each direction depends on the cross section. The total number of cells in the initial grid is 174 312 which after adaption becomes 216 375 cells. The adaption is performed on geometrical basis refining the grid in areas where the fire source and assumed plume are located. After adaption the average cell volume is about 1 m^3. The cell volume range is 0.0116…13.33 m^3. Near the fire source and in the adapted areas the cell volume is at the smallest.

The surface grid of the hall is shown in Figure 1. In unit 1 near turbine number 2 the grid is locally refined which can be seen from the figure.

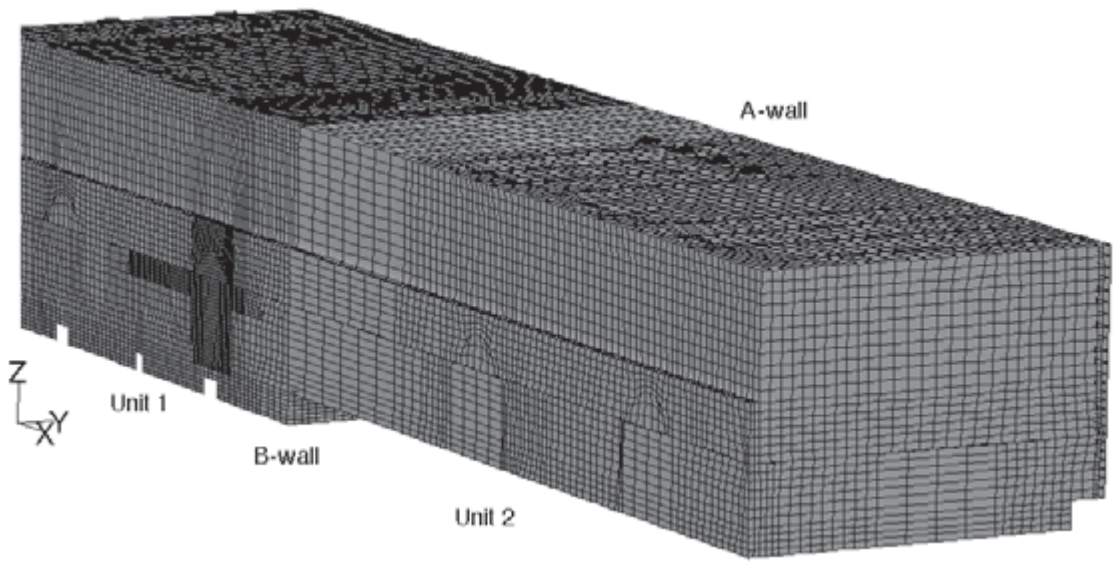

Figure 1. *Hall seen from the B-wall side. The surface grid gives a clue about the computational grid. The grid has been refined near the turbine #2 on unit 1 side.*

3.2 Ventilation

The nominal ventilation rate is 92 m^3/s on both units. The ventilation is applied when needed. In the simulation it is assumed that the ventilation operates at the nominal rate all the time. The total modelled volume of the hall is 220 566 m^3. With the nominal ventilation rate the whole air content is changed in 20 minutes. The assumed simulation time is of the same order so ventilation may have a remarkable influence in the temperature field.

Air is blown in from several nozzles on the A-line wall. Nozzles are located on the levels +19.00 and +6.00 and under the level +3.00. In the model the nozzles under the level +3.00 in unit 2 side are lifted up because the lowest modelled level on that side is +3.00.

Air outflow takes place in twelve outlets at the ceiling (on both units) near the B-line wall. The openings are equipped with fans that balance the pressure difference in the hall. The outlets are modelled as pressure outlets. Two openings are connected together in the model, because outlets are located in pairs side by side. In a fire there is doubt about the temperature tolerance of the outlet fan electric motors. The maximum design temperature for the continuous operating of the motors is 40°C. In simulation it is assumed that the outlets are not blocked due to the fans but stay open all the time.

According to the emergency instructions (KÄ4 535/M3) all the smoke hatches are opened manually at once a fire in the turbine hall is detected. In the simulation the smoke hacthes are opened separately as soon the temperature under each hatch has reached the threshold value. In Figure 2, the inside of turbine hall is shown. Fresh air inlets, ventilation outlets and smoke hatches are shown as well.

It is also possible to open the row of windows on the upper edge of wall A to enhance the ventilation. In the simulation it is assumed that the windows are closed and they are not broken during the simulated time.

3.3 Oil pool formation

Oil pool formation is set as a predefined scenario where the spread velocity and total pool area are defined á priori. The total pool area is 75.6 m^2. The dimensions of the pool on cable tunnel 3 are given in Figure 3. The part of the pool on the side of the condenser has the same dimension in the x-direction as tunnel 3 (3.5 m). The height of the condenser is 9.6 m. With the assumed maximum vaporization rate of oil this gives about 150 MW of maximum burning rate. The burning rate is not defined as a boundary condition, but the corresponding amount of fuel is released from the pool.

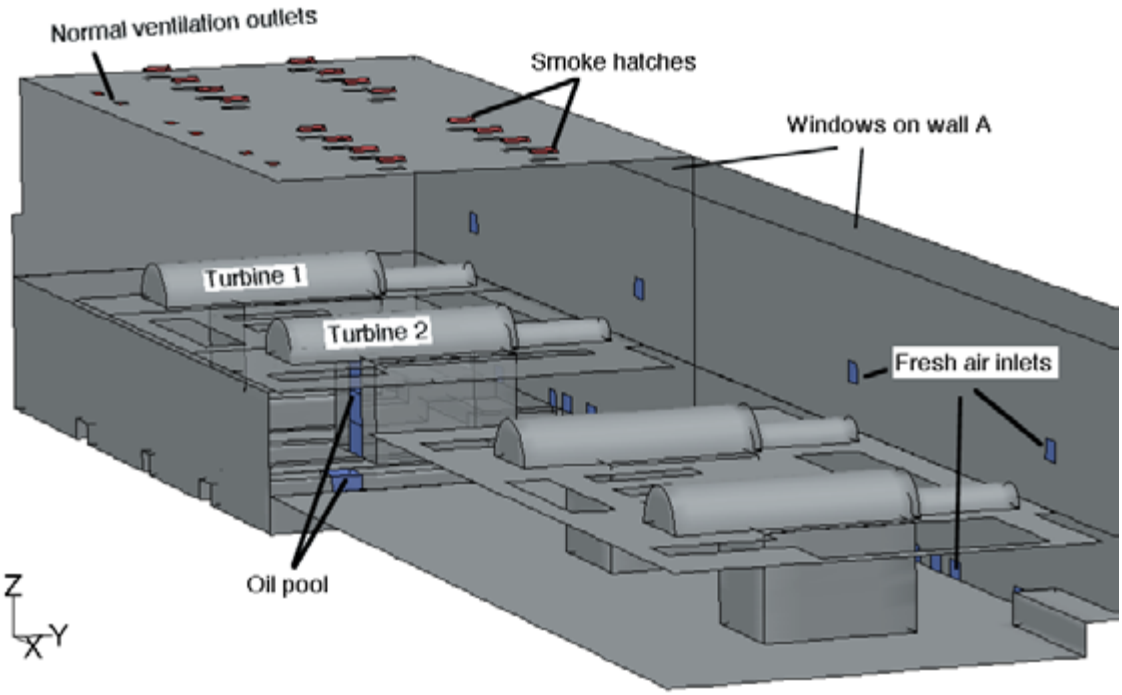

Figure 2. *Inside of the turbine hall. Some intermediate decks are removed from the picture for clarity. Fresh air inlets and ventilation outlets are shown.*

The fuel burns then according to EBU-model, which takes the turbulence and species concentrations into account. Other burning material like cable insulation is not taken into account. This is assumed to have generally small effect to the heat load, although it may locally have some influence. Also any fire suppressing actions are not taken into account.

It is assumed that oil leak takes place at the high–pressure end of the turbine no. 2 at unit 1. At the same occasion oil is ignited and it has access through the turbine bed down to the lower levels. Oil is assumed to flow down on the wall of the condenser unit under the turbine. The turbine is located on level +12.60 m. The condenser comes down to the level +3.00 m. On that level there is a gap between the condenser and the floor (about 1 m wide) where the oil spreads down to the cable tunnel below and further to the level –0.60 m. The assumed spread velocity is 0.15 m/s both downwards and in horizontal direction. The heat of combustion for the oil is 42.8 MJ/kg. The maximum fuel release rate corresponds to the burning rate of 2 MW/m^2. With the oil density of 865 kg/m^3 the corresponding oil regression rate is 3.3 mm/min (or 4 liters/s). In the combustion model practically all released oil is burned, thus this represents the effective fuel release rate.

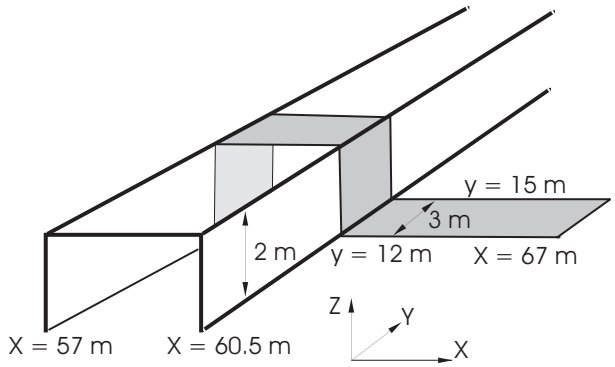

Figure 3. *Oil pool (shaded area) around cable tunnel 3 and on the floor –0.60 m.*

Figures 4 and 5 show the turbines 1 and 2 and the oil pool under turbine 2. Oil pool is formed on the cable tunnel number 3 and on the level –0.60 m. After this basic scenario also an optional fuel release rate was calculated. In this option the fuel release rate corresponded to 200 MW of fire rate. The fuel flow was increased from the nominal value to the new maximum after 12 minutes from the ignition.

3.4 Smoke hatches

There are 32 smoke hatches on the roof of the turbine hall. They are like small huts with a roof, which can be opened. The roof is operated with pressure actuators when temperature under the hatch rises to 120°C (393 K). The smoke hatches are opened separately and independently, but they can also be opened manually. The dimensions of the hatch opening are 2.5 m · 1.2 m.

In the simulation the hatches are opened after the temperature has reached the threshold value. The same pressure outlet boundary condition is applied to these as in the normal ventilation outlets. The operation is not automated in the code but the boundary conditions are changed manually after the threshold has been reached.

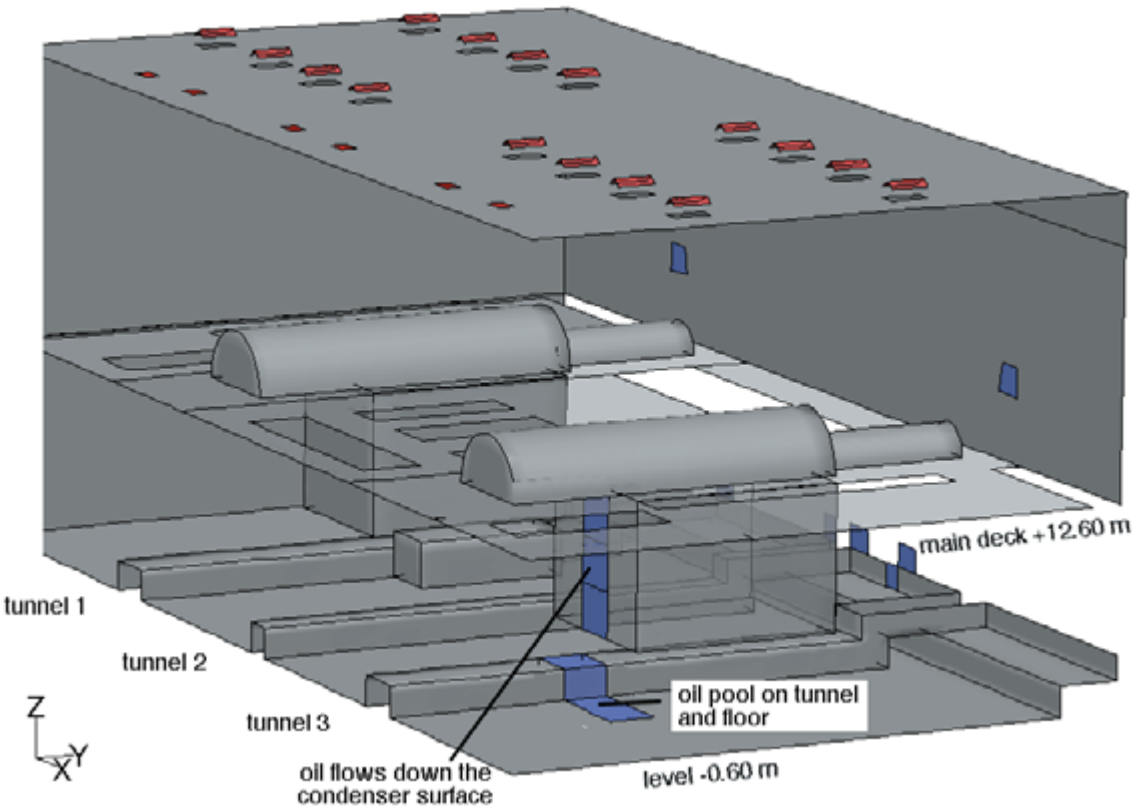

Figure 4. *Hall, unit 1 turbines 1 and 2. Some intermediate decks are removed for clarity.*

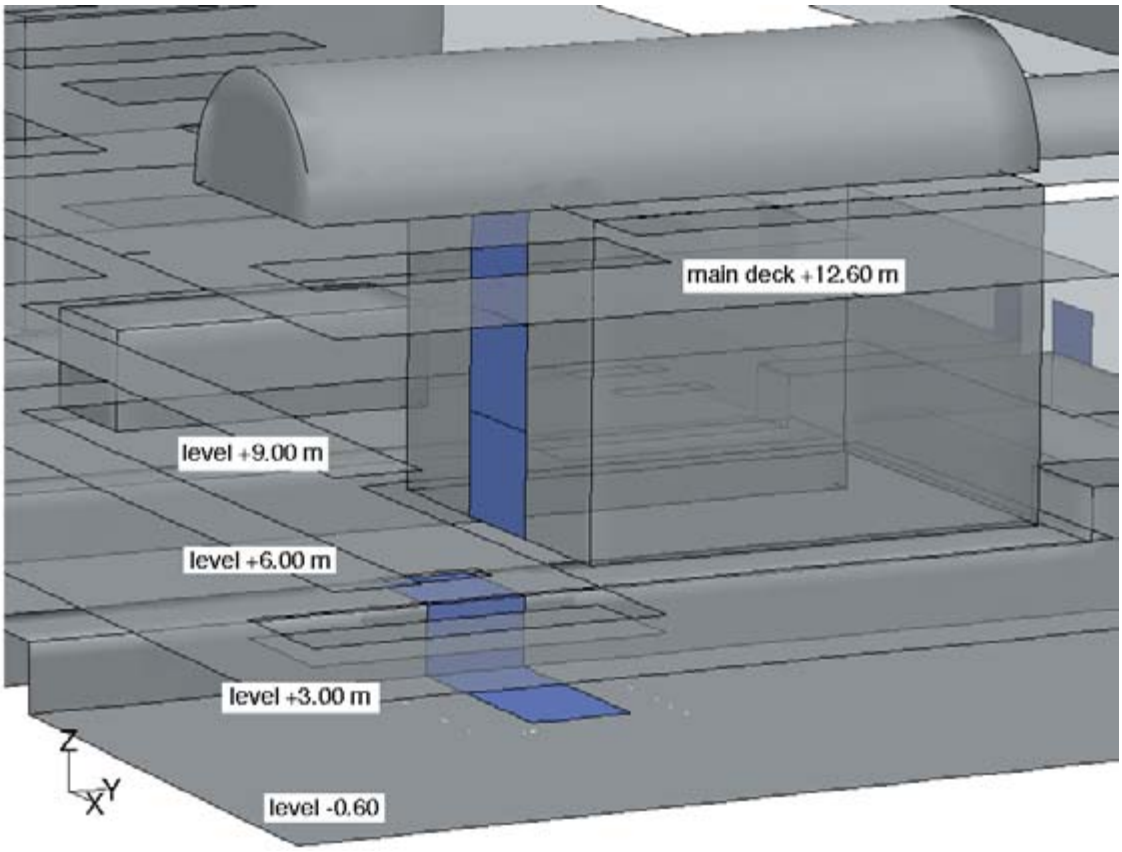

Figure 5. *Detail in the oil pool area. Some structures are drawn transparent.*

4 Simulation

4.1 Initial conditions

The initial conditions, i.e. the normal flow and temperature fields are calculated before the actual fire simulation is started. The nominal ventilation rate is applied. It is assumed that the temperature of the incoming air is 15°C (288 K). The heat sources in the hall (turbines, generators, main feed water pumps, …) are partly defined as heat sources, partly the heat source is distributed to cover the total normal heat release from these objects. The initial state is calculated to a steady situation. The initial temperature field is given in Figure 6. The same cross sections (x = 58.75 m and y = 14 m) are used also in temperature field animations.

4.2 Beginning of fire with closed hatches

At the initial stage of the fire, the smoke hatches and windows on A-line wall are all assumed to be closed. The ventilation is operated at the nominal flow rate. Oil is ignited immediately when it starts to spread. It is assumed that the fire source is located under the main deck +12.60 m even though it is possible that oil can spread also on the deck. The simulated temperature field on cross sections x = 58.75 m (abeam turbine #2) and on cross section y = 14 m (abeam the first row of smoke hatches) are given in Figures 7 and 8. During simulation a series of pictures are drawn to form an animation of the temperature development.

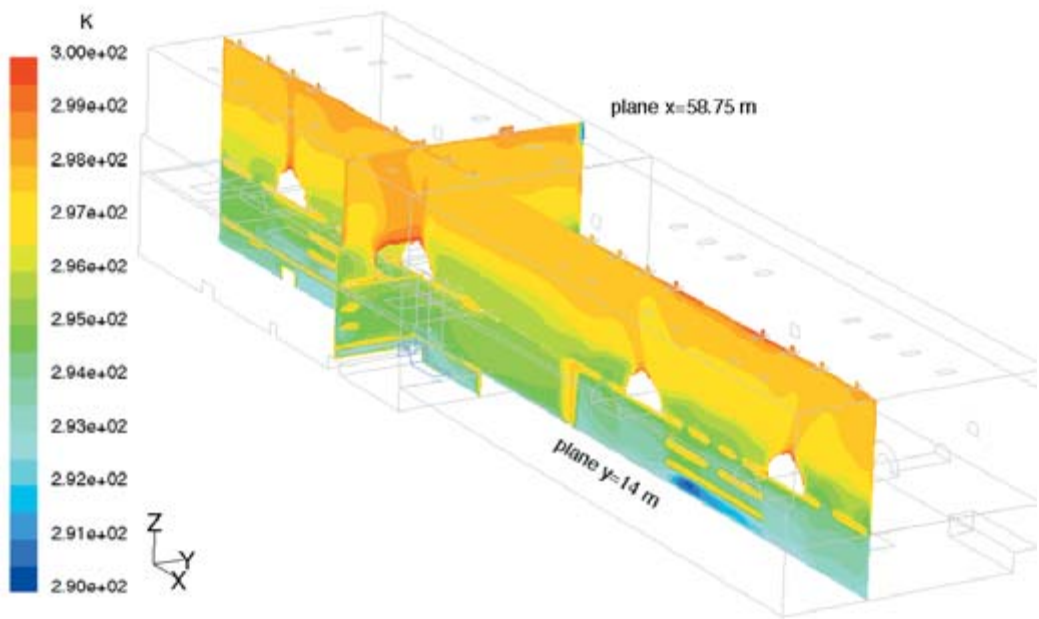

Figure 6. *Initial temperature field on cross sections x = 58.75 m (abeam turbine no. 2) and y = 14 m (abeam the first row of smoke hatches).*

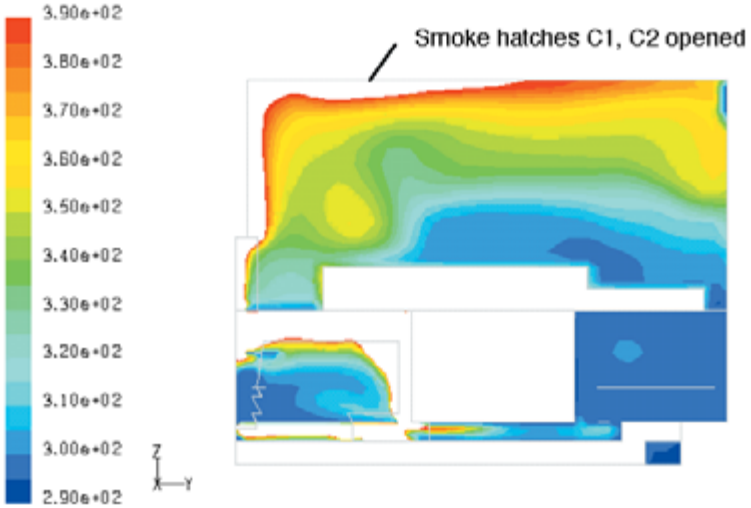

Figure 7. *Temperature field on cross section x = 58 m at 300 seconds from ignition. The temperature range shown is 290…390 K (17…117°C). The threshold temperature for smoke hatches to operate is 393 K (120°C). At this stage the smoke hatches C1 and C2 are opened. The area beyond the red colour denotes temperature higher than the range limit.*

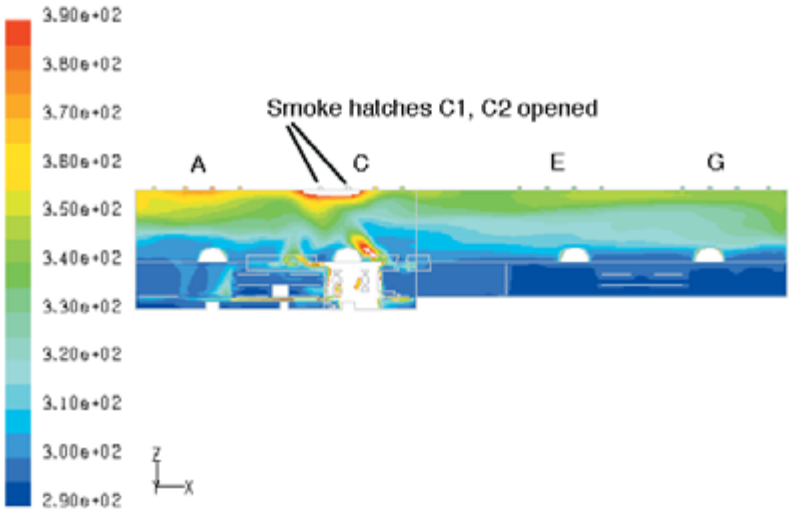

Figure 8. *Temperature field on cross section y = 14 m at 300 seconds from ignition. The area beyond the red colour denotes temperature higher than the range limit.*

4.3 Fire with opening hatches

The modelled 32 smoke hatches on the roof are located in the groups of four. The threshold temperature of opening is 393 K (120°C). From Figure 9 it can be seen that the temperature is higher than the threshold value under hatches C1 and C2. The hatches are operated individually and independently, but can also be controlled manually. In the simulation the hatches are opened after the threshold temperature is reached. This takes place by changing manually the boundary conditions and proceeding from a proper situation using the nearest restart file. The data-files for restart are saved every ten seconds. The time steps to open the hatches in the simulation are shown in Table I. The layout and labeling is shown in Figure 10. In each group the hatches are numbered form 1 to 4 from left to right as shown in the figure.

Table I. *Time steps to open the hatches during the simulation. The hatch is opened when the threshold value of temperature is reached under the opening..*

Time [s]	Event
300	C1, C2 opened
370	C3, D2 opened
400	A4, D3 opened
440	A3, B3 opened
480	A1–2, B1–2, B4, C4, D1, D4 opened (all hatches on unit 1 side are open)
540	F1–4 opened
580	H1–2, E3–4, G1 opened
600	H3–4, G2–3 opened
620	E1–2, G4 opened (all hatches on both units are open)

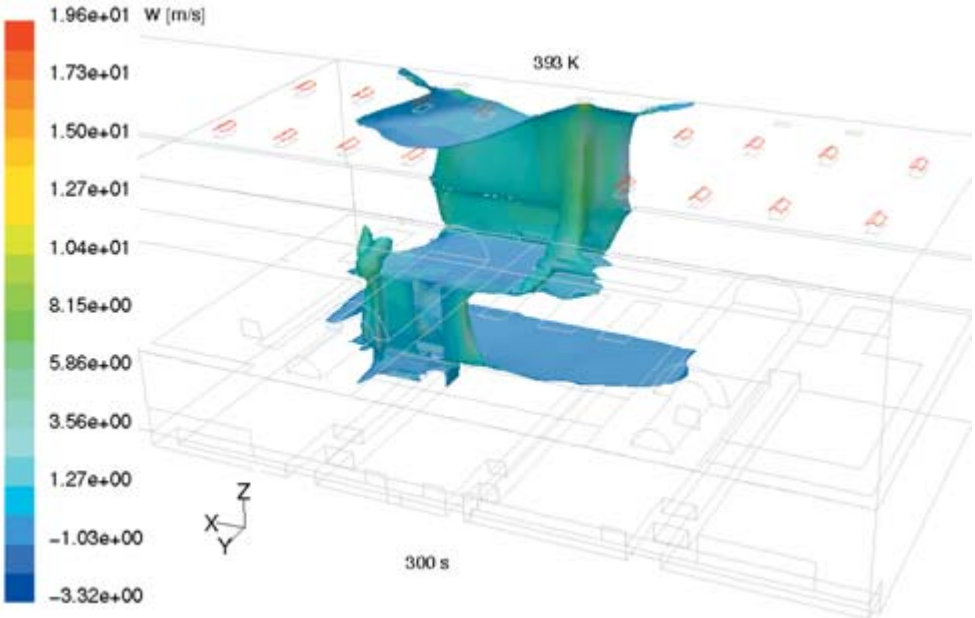

Figure 9. *Temperature contour 393 K (120°C), coloured by the vertical velocity, above the fire source at 300 seconds from ignition. Under the ceiling the plume is divided into two jets with flow direction about 45 degrees from the normal of the B-wall.*

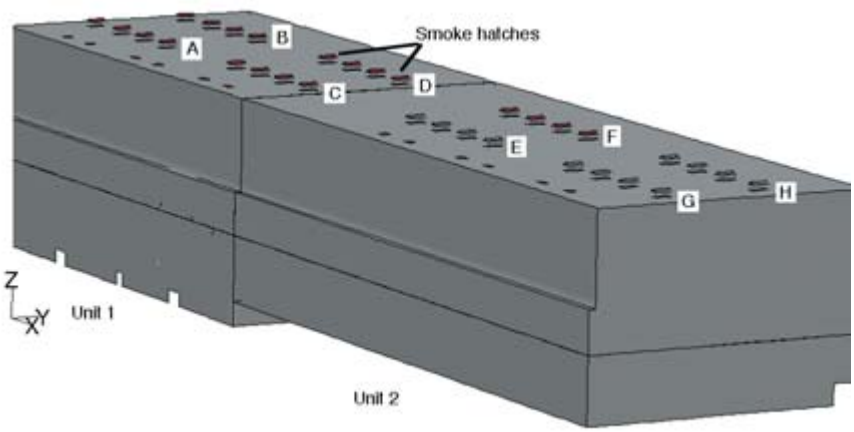

Figure 10. *Smoke hatches on the roof. Numbering of hatches goes from left to right (f.ex. C1, C2, C3, C4).*

The temperature history under the hatches is shown in Figure 11. The presented temperature value is the maximum temperature under the four hatches in a group. The temperature is rising even after 20 minutes although the temperature change is not so rapid as in the first minutes. The maximum gas temperature under the hatches A–D at this stage is about 220°C (493 K). The presented value is a local one and there may be found also higher temperatures in locations where the plume hits the ceiling.

The chemical reaction rate is presented in Figure 12. The small variation in the reaction rate is caused by the fluctuations of the flow and concentration fields. Finally practically all the released fuel is burned. The total amount of burned fuel after five minutes is 480 kg and after that the release rate is constant 3.55 kg/s. At 20 minutes the total consumption is 3 678 kg. The total amount of oil in the lubricating system is 56 m³, about 48 440 kg. The volume of gravity oil tanks is 2 · 8.5 m³.

4.4 Temperature field

The temperature field at different time steps is shown in Figures 13–16. The oil pool fire has

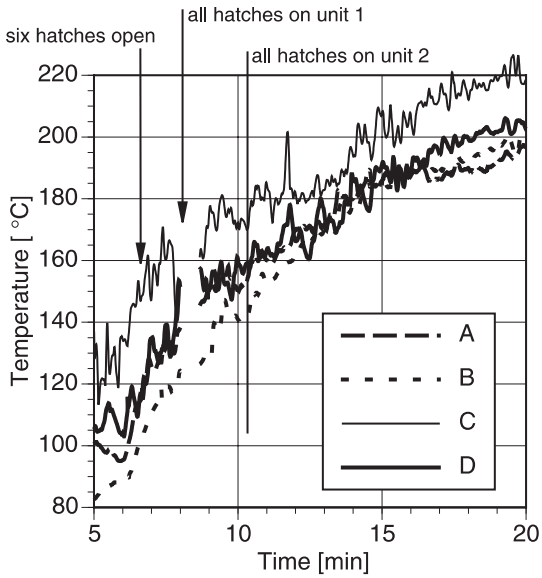

Figure 11. *Maximum temperature under hatches A–D. All hatches on unit 1 side are open after 8 minutes and on both units after 10 minutes 20 seconds.*

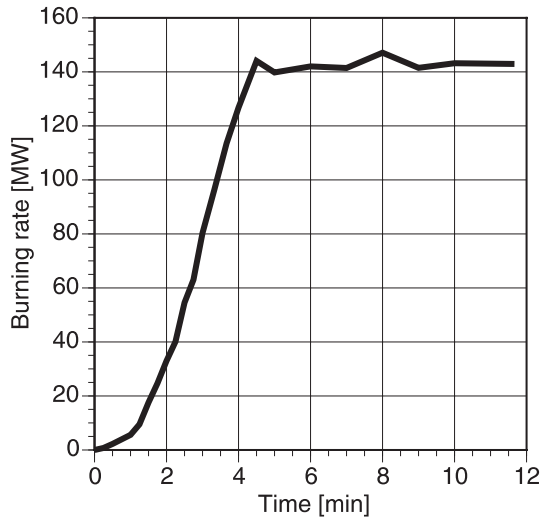

Figure 12. *Chemical reaction rate during the fire according to EBU-model.*

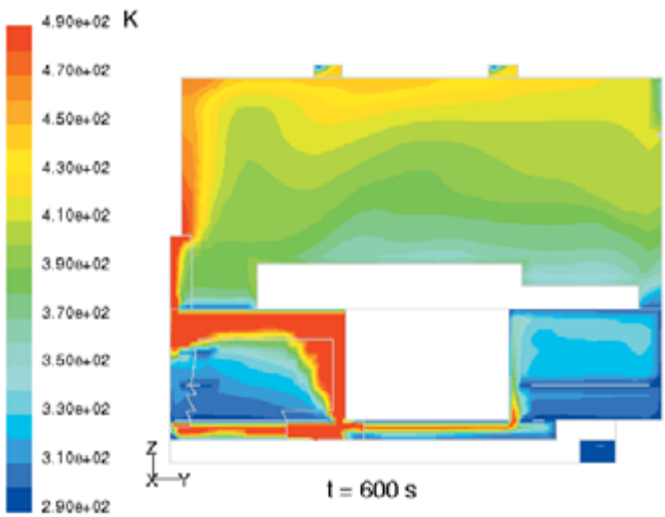

Figure 13. *Temperature field on cross section x = 58.75 m at 600 s from ignition. The red colour denotes 490 K and higher temperature.*

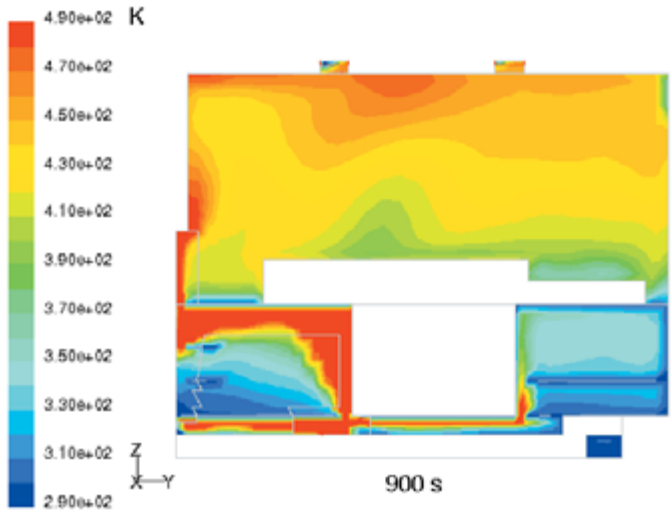

Figure 14. *Temperature field on cross section x = 58.75 m at 900 s from ignition.*

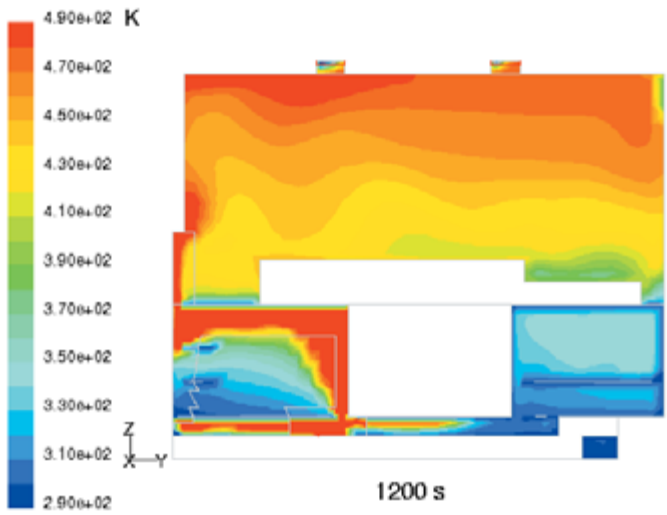

Figure 15. *Temperature field on cross section x = 58.75 m at 1200 s from ignition.*

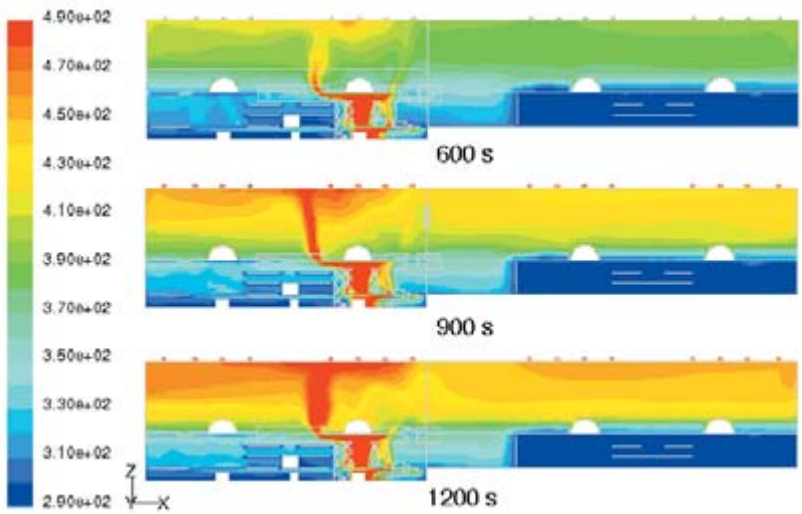

Figure 16. *Temperature field on cross section y = 14 m at 600 s, 900 s and 1200 s from ignition. The red colour denotes 490 K and higher temperature.*

reached its maximum heat release rate in five minutes (Figure 12) and the smoke hatches start to open just thereafter (Table I). The iso-temperature contours of 393 K (120°C) are shown in Figures 17–22 and temperature contours of 473 K (200°C) in Figures 23 and 24.

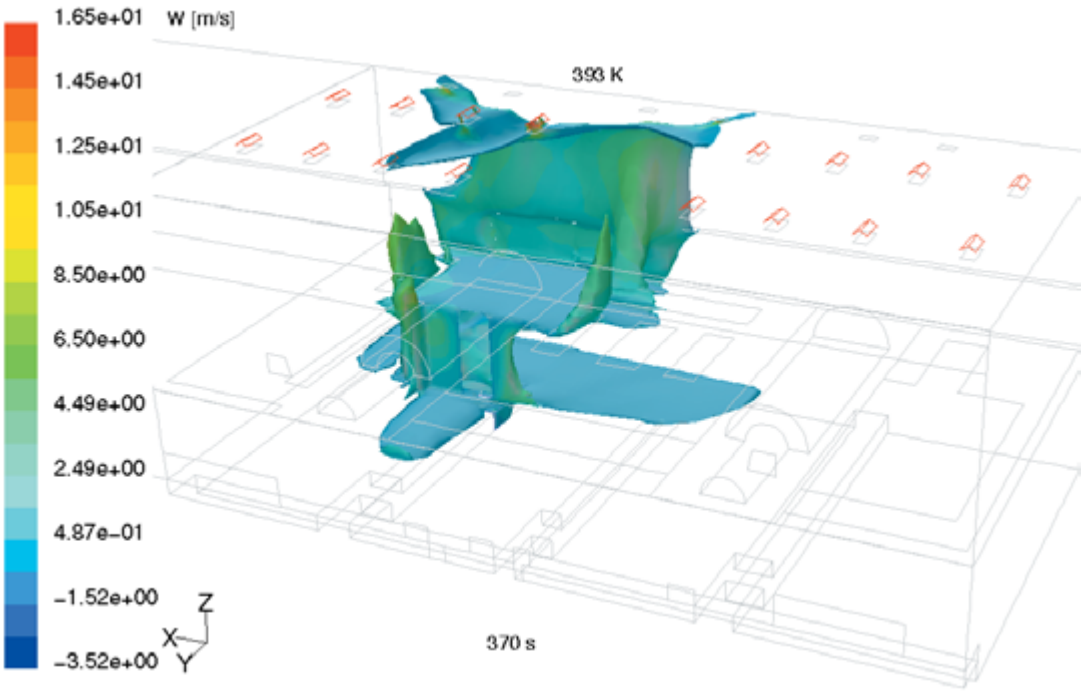

Figure 17. *Temperature contour 393 K (120°C) above the fire source at 370 seconds from ignition.*

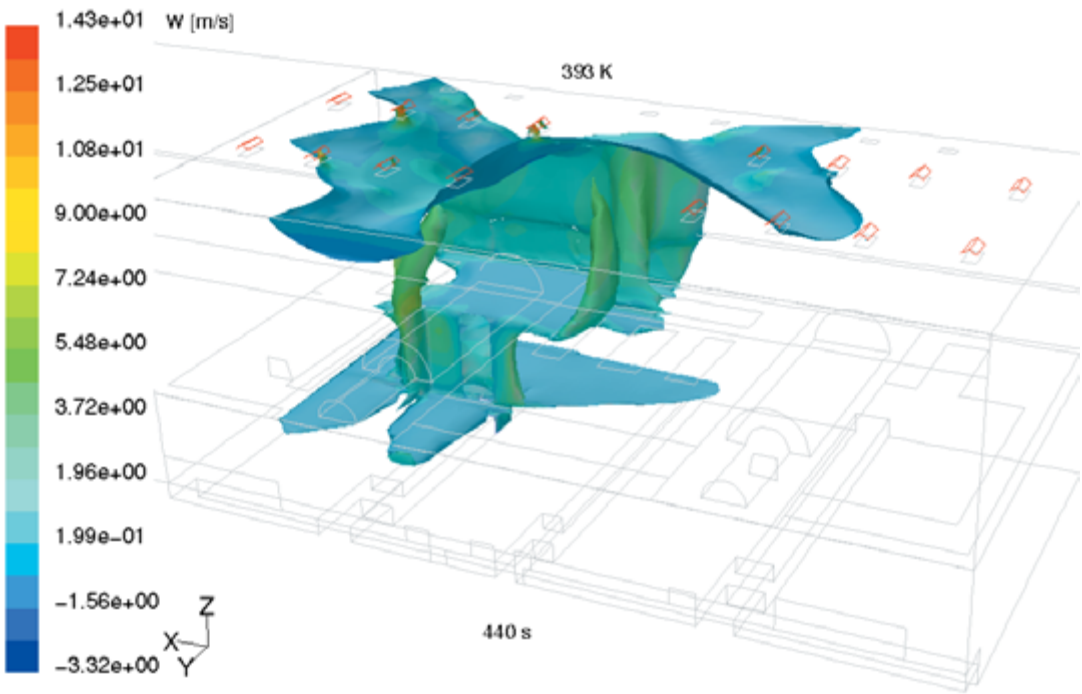

Figure 18. *Temperature contour 393 K (120°C) above the fire source at 440 seconds from ignition.*

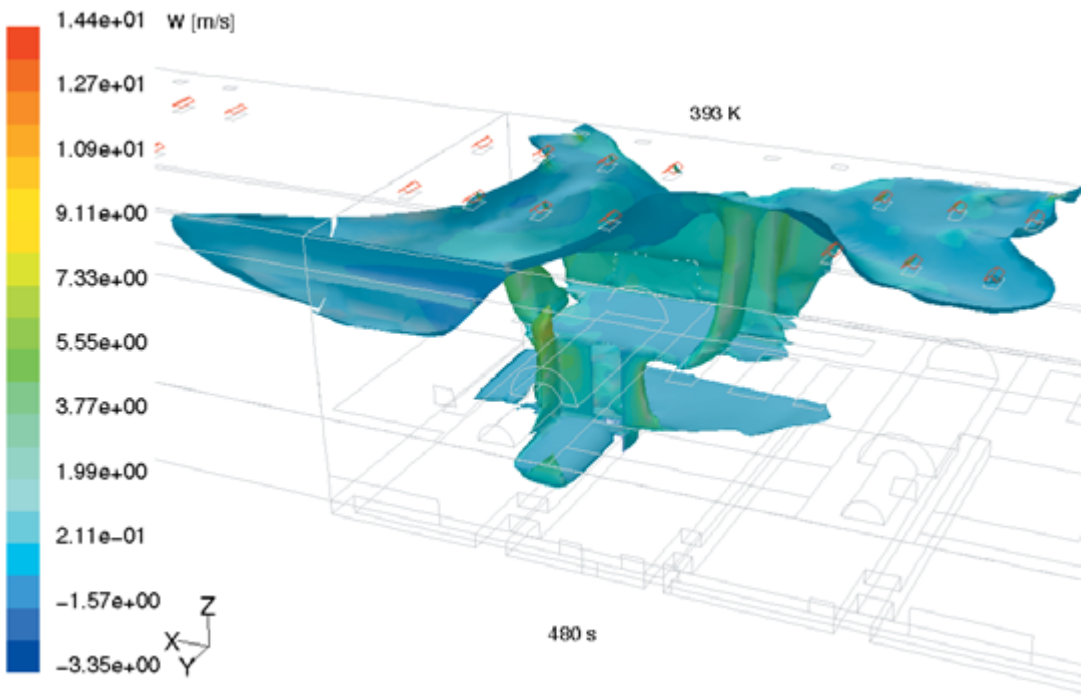

Figure 19. *Temperature contour 393 K (120°C) above the fire source at 480 seconds from ignition.*

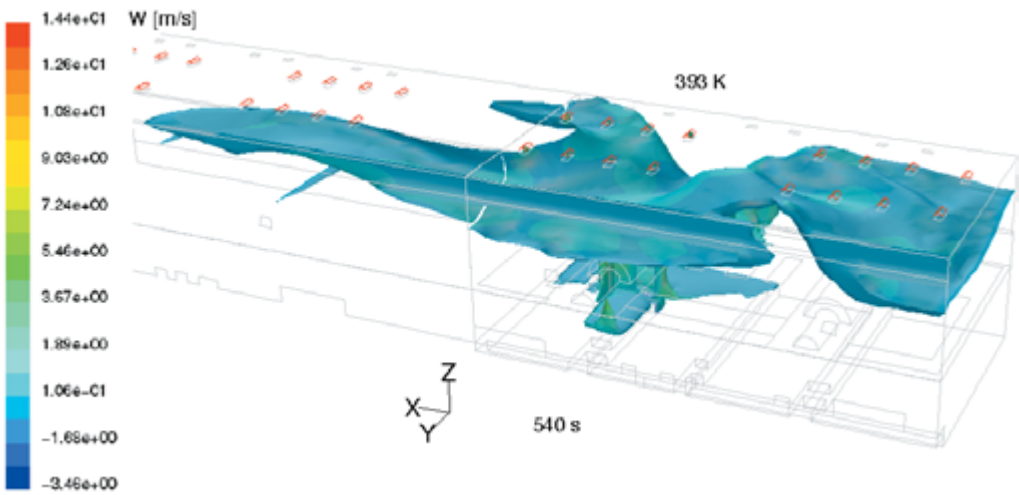

Figure 20. *Temperature contour 393 K (120°C) above the fire source at 540 seconds from ignition.*

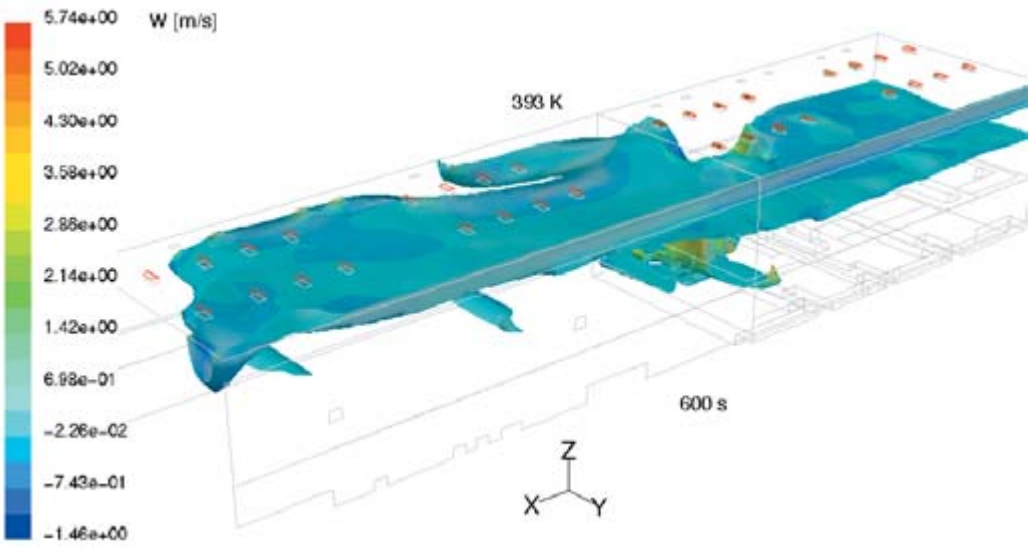

Figure 21. *Temperature contour 393 K (120°C) above the fire source at 600 seconds from ignition.*

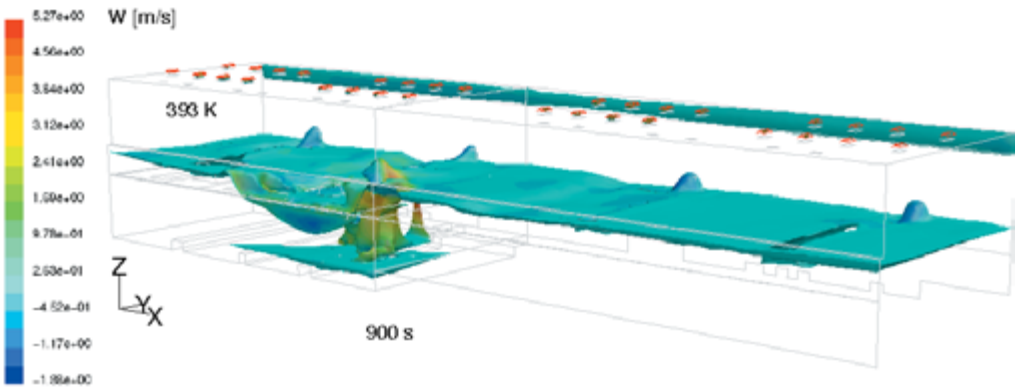

Figure 22. *Temperature contour 393 K (120°C) above the fire source at 900 seconds from ignition. The view is taken from the B-wall direction. the fresh air inlets are shown as 'bumps' on the surface near the A-wall.*

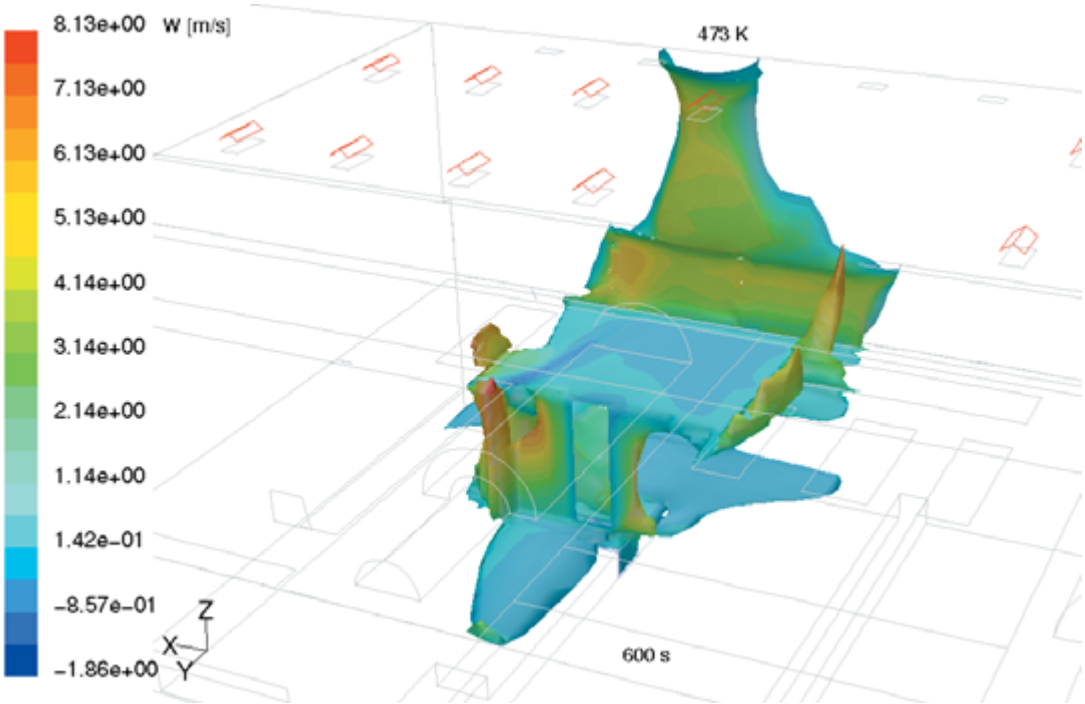

Figure 23. *Temperature contour 473 K (200°C) above the fire source at 600 seconds from ignition.*

4.5 Incident radiation to the structures

The highest radiation fluxes are found in the flame and plume area. The burning seems not to be limited by oxygen supply at any stage, because the building is so large and open to the lowest level. When the pool has been spread over tunnel 3, the structure can be considered surrounded by flames. The other walls and neighbouring cable tunnels are effected by different heat loads depending on their orientation to the flame and the plume. Figures 25–32 present the incident radiation heat flux to different walls.

According to this simulation, it seems that the neighbouring tunnels on level –0.60 m are not effected by very high radiation fluxes. The plume has been stabilized to follow the surface of the

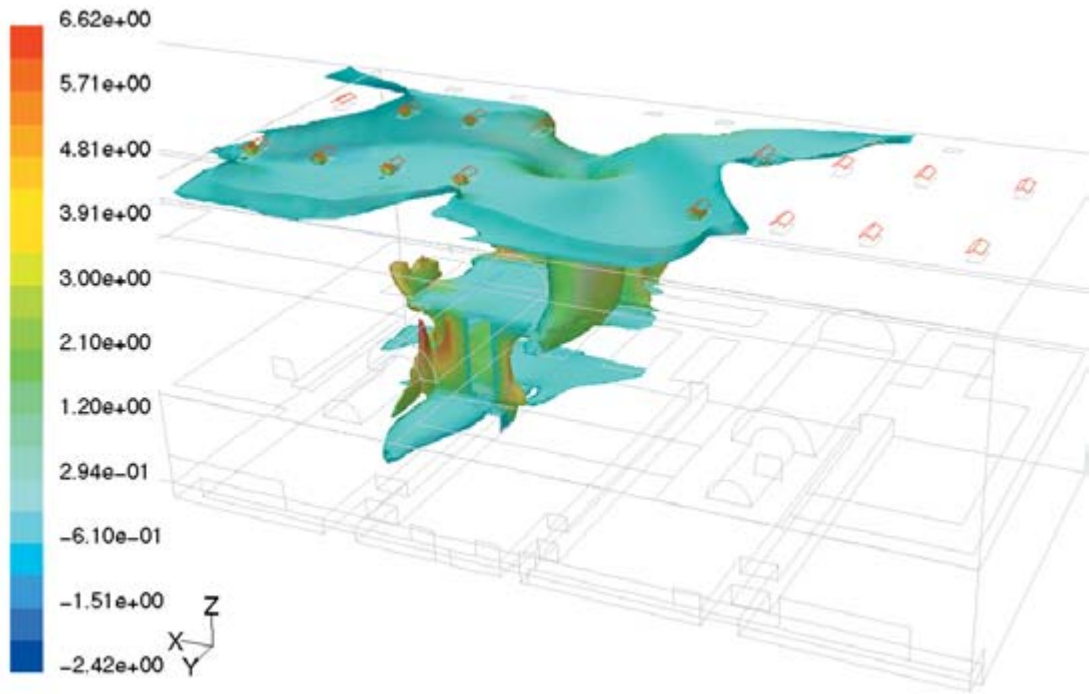

Figure 24. *Temperature contour 473 K (200°C) above the fire source at 1200 seconds from ignition.*

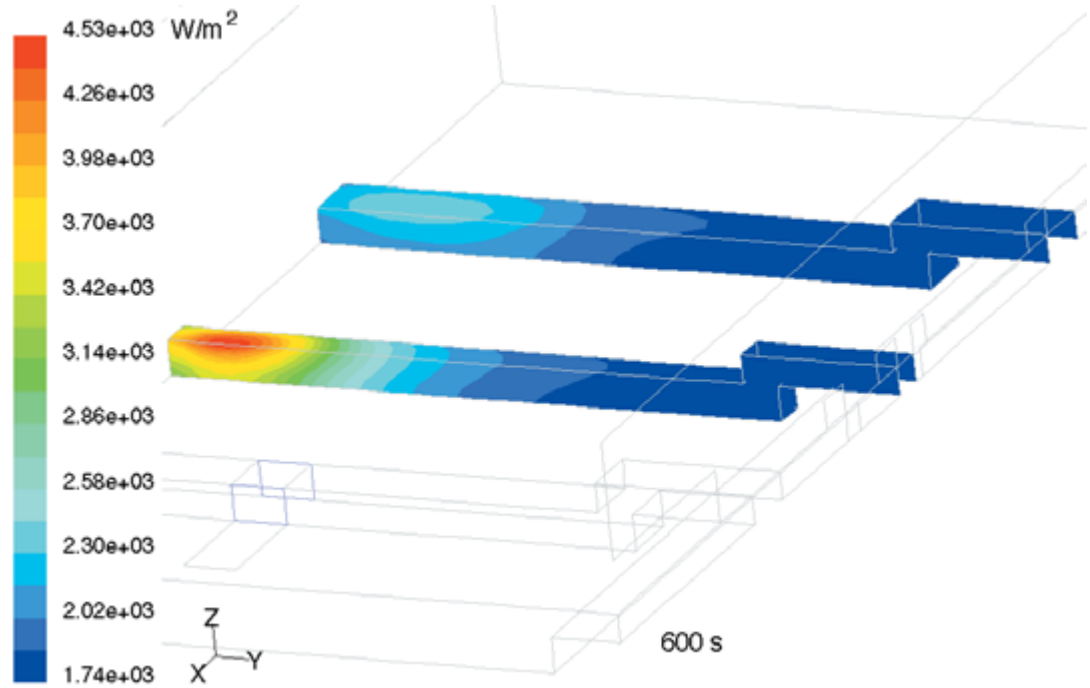

Figure 25. *Incident radiation flux to the cable tunnels 1 and 2 on the level –0.60 at 10 minutes from the ignition.*

heat exchanger and that flow route is the most favorable to hot gases. The part of the hot gases that spreads under the level +3.00 finds its way rather quickly to the upper levels also through the other openings. Thus the hot layer under the level +3.00 m is not growing very thick.

The situation near tunnel 4 (Figures 26 and 30) depends very much on ventilation, if it is on or

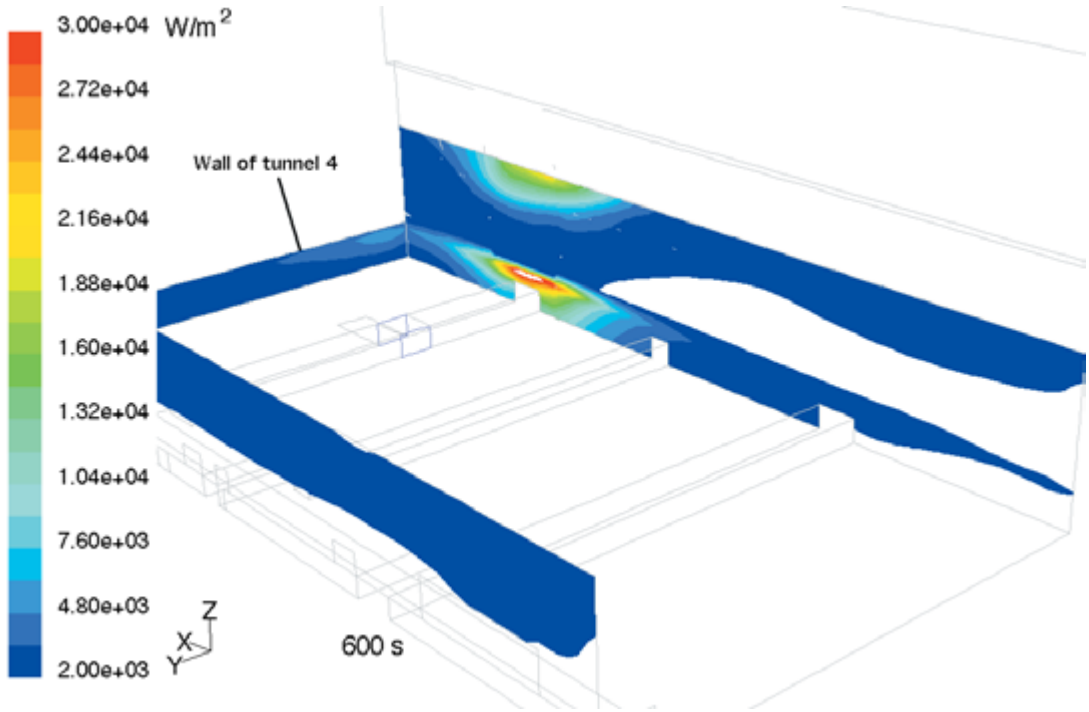

Figure 26. *Incident radiation flux to the cable tunnel 4 and wall B on the level –0.60 at 10 minutes from the ignition.*

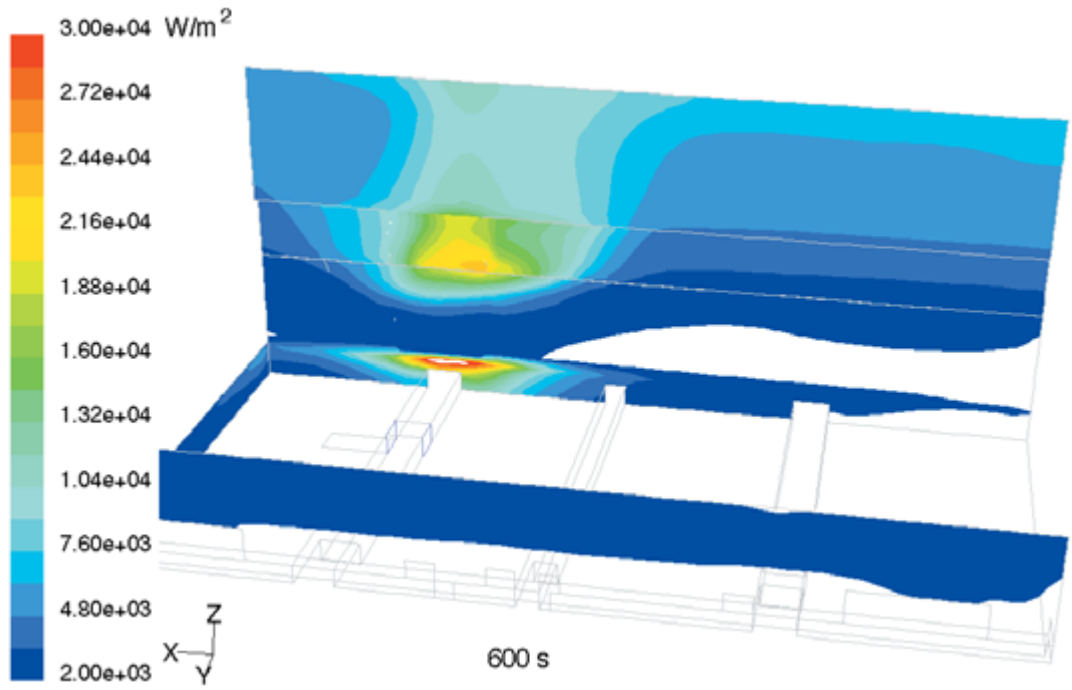

Figure 27. *Incident radiation flux to the B-wall on the level –0.60 to +32.50 m at 10 minutes from the ignition.*

not. In this simulation, the ventilation is operating at the nominal rate giving cool air to the area. The location of tunnel 4 is next to tunnel 3. The tunnel itself is outside the computational grid. Only the wall is seen.

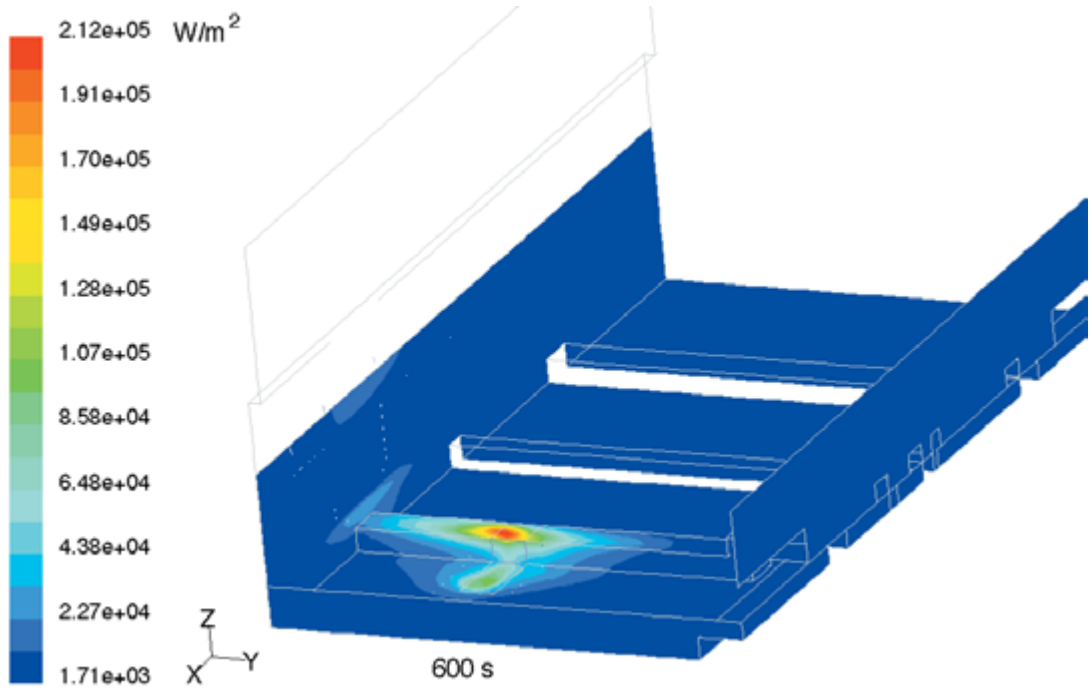

Figure 28. *Incident radiation flux to the cable tunnel 3 and the floor on the level –0.60 at 10 minutes from the ignition.*

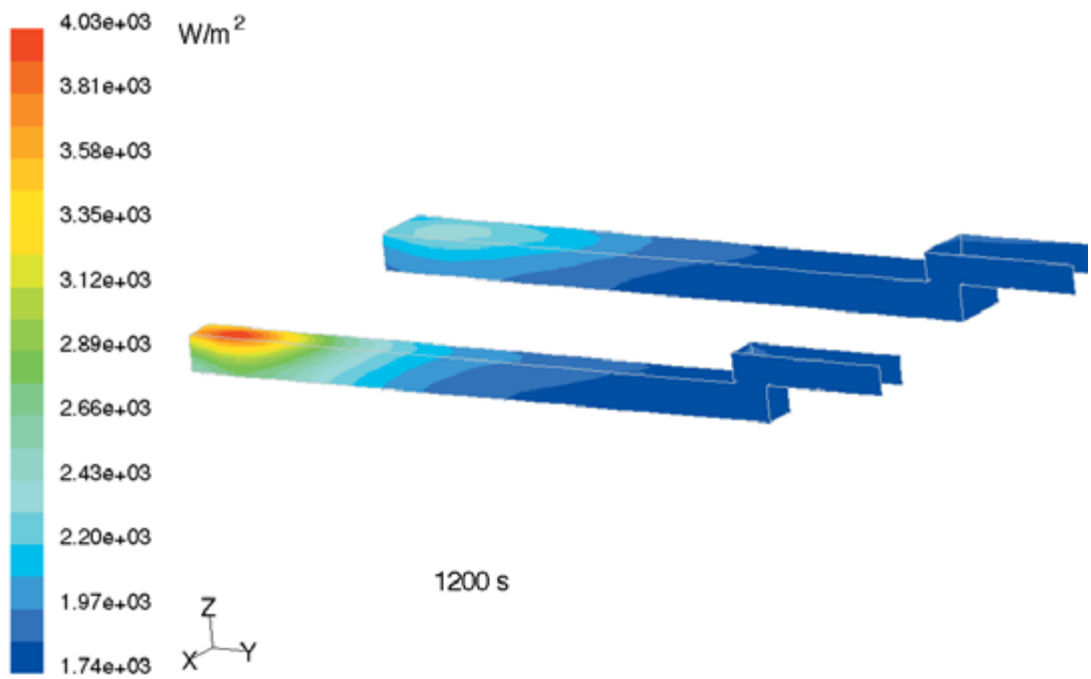

Figure 29. *Incident radiation flux to the cable tunnels 1 and 2 on the level –0.60 at 20 minutes from the ignition.*

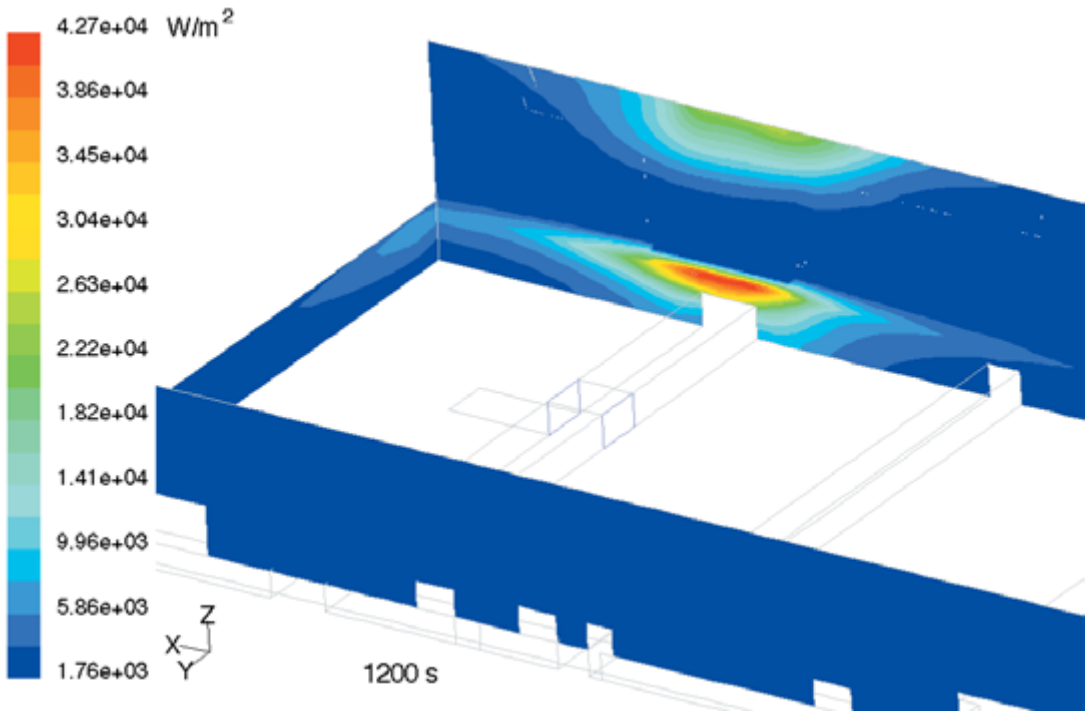

Figure 30. *Incident radiation flux to the cable tunnel 4 and wall B on the level –0.60 at 20 minutes from the ignition.*

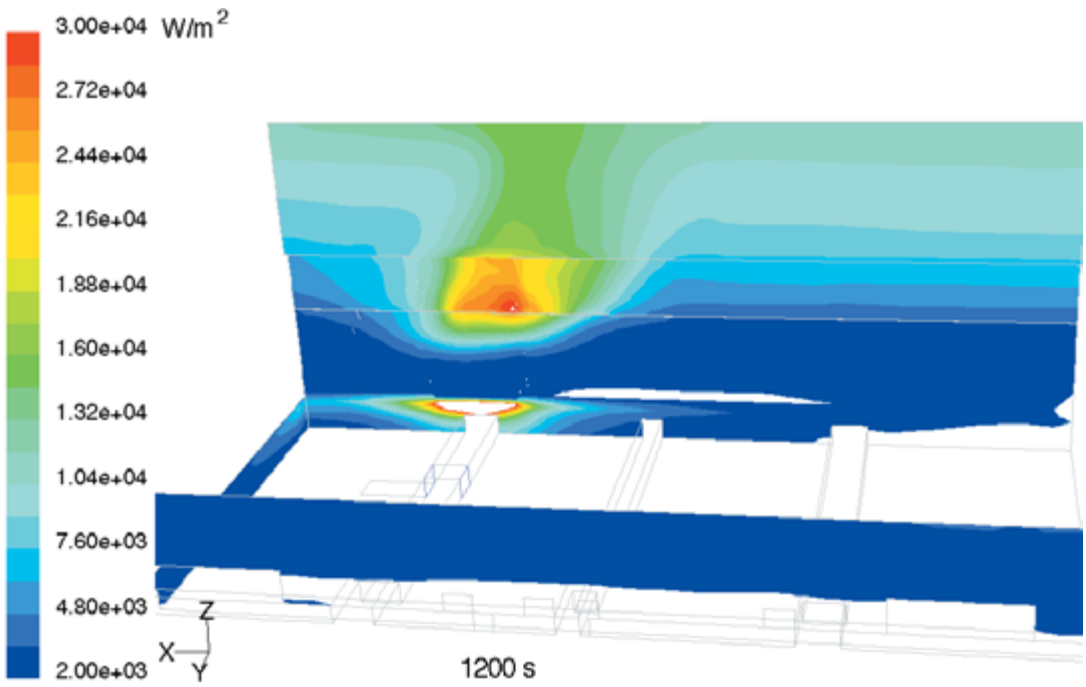

Figure 31. *Incident radiation flux to the B-wall on the level –0.60 to +32.50 m at 20 minutes from the ignition.*

4.6 Gas temperature near the structures

The heat load depends both on radiation and convection. The fluid temperature near the structures is given with profiles in Figures 33–35.

The local temperature profile near the tunnels 2 and 4 is given in Figure 33. The vertical profile is from 0.5 m from the tunnel surface and 3 m from B-wall. The location is taken from the maximum temperature area. The tunnels span from the level –0.60 m to the level +1.40 m, while

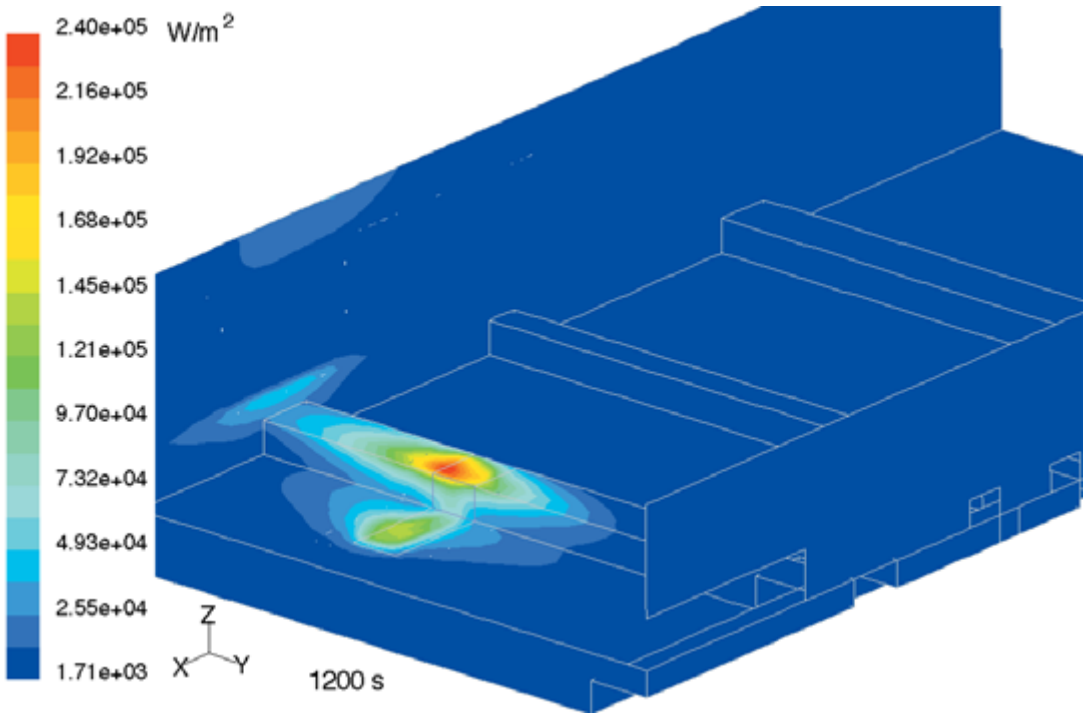

Figure 32. *Incident radiation flux to the cable tunnel 3 and the floor on the level –0.60 at 20 minutes from the ignition.*

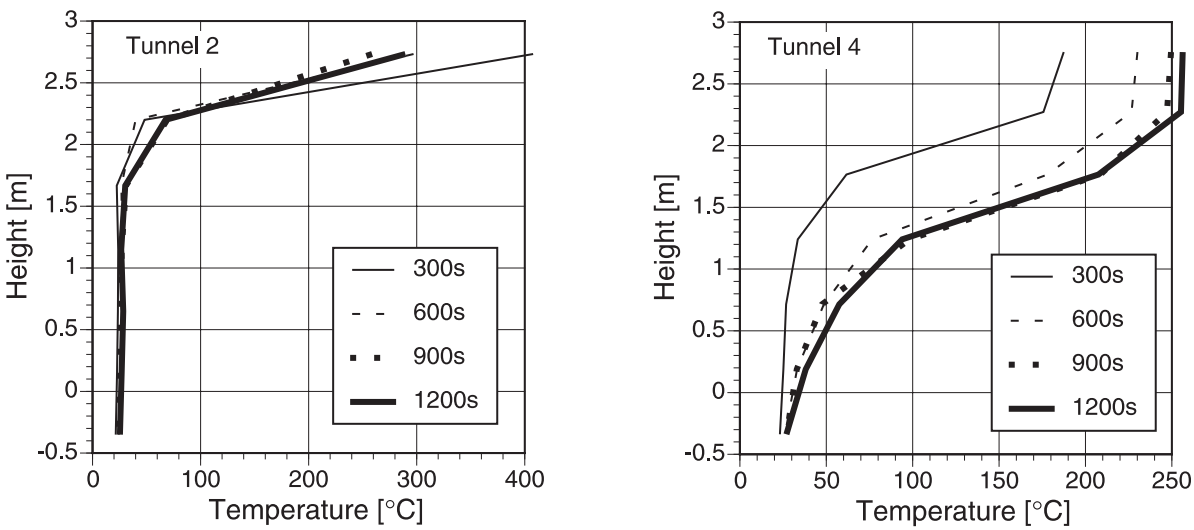

Figure 33. *Gas temperature near the tunnel 2 and tunnel 4 at different time steps. The profile is taken at 0.5 m from the tunnel wall and 3 m from the B-wall.*

tunnel 4 spans close to the upper floor on level +3.00 m. The ceiling is on the level +3.00 m.

Temperature profile near B-wall is shown in Figure 34. The location of the profile is abeam the fire and 1.5 m from the B-wall. The distance is chosen so that the whole height of the hall is taken to the profile (B-wall makes a kink of one meter on the level +19.00 m). The maximum temperature under the level +3.00 is very high (even 750°C) due to the flame area (Figure 34). On floor level (–0.60 m) the temperature keeps low due to the cool air circulation and ventilation. The concrete deck separates the volume very well and temperature above level +3.00 m remains in moderate values until to the plume under the main deck on level +12.60 m. The plume area is about +9.00…+12.60 m where the auxiliary deck partially restricts the temperature rise under the level +9.00 m. Above the main deck the plume mixing is stronger and the plume temperature is reduced. The maximum temperature of the plume when hitting the B-wall under the main deck is about 450°C.

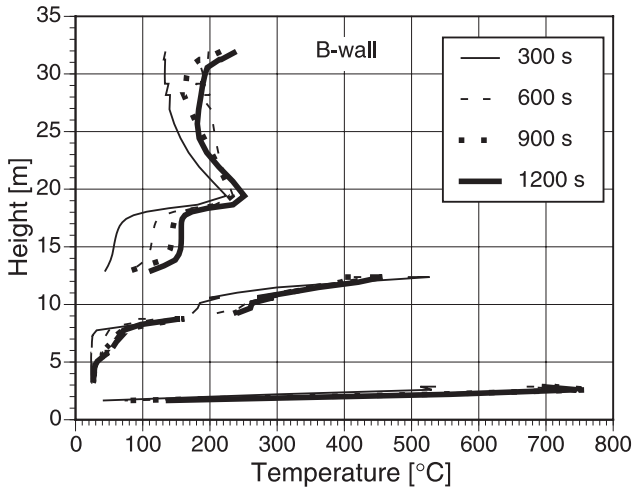

Figure 34. *Gas temperature near the B-wall at different time steps. The profile is taken at 1.5 m from B-wall abeam the fire source.*

The general temperature profile in the turbine hall is given in Figure 35 at the middle of the hall and between the turbines 1 and 2 in the main deck opening. The maximum temperature below the ceiling at 20 minutes is about 220°C on the unit 1 side between turbines 1 & 2 and about 190°C at the middle of the hall.

The temperature field under the ceiling at different time steps is given in Figure 36 and Table II. The range in Figure 36 is taken on level +32.00, i.e.0.5 m below the ceiling.

Temperature range near B-wall is given in Figure 37 and Table III. The shown plane is 0.5 m from the B-wall. The highest temperature is found below the level +3.00 m. Local maximum is found at level +12.60 m where the plume passes the edge of the main deck. The hot layer under deck +3.00 is not very thick.

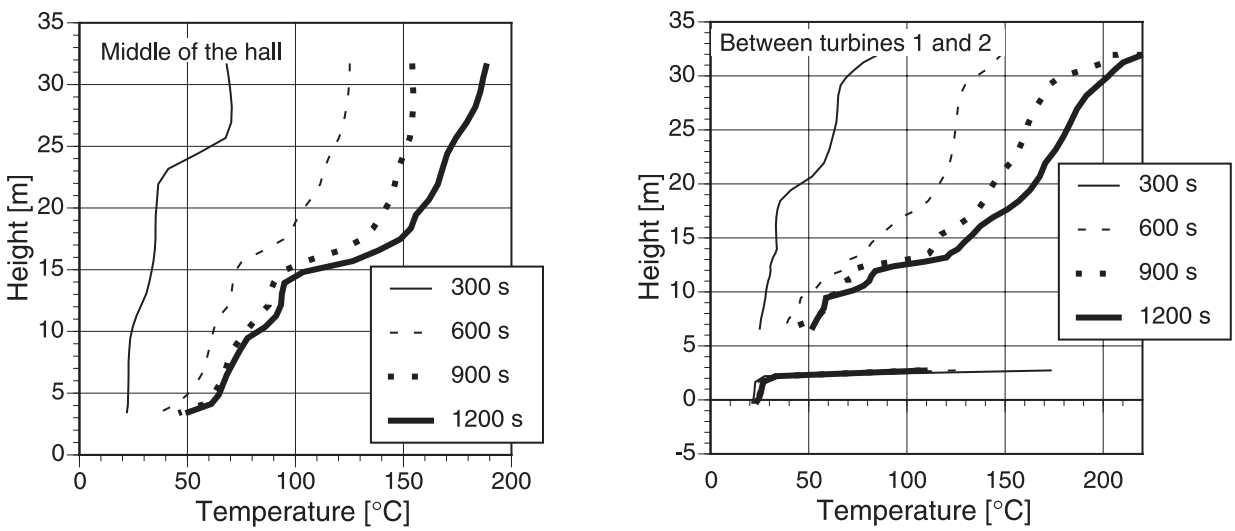

Figure 35. *Gas temperature profiles at the middle of the hall (x = 90 m, y = 21 m) and between turbines 1 and 2 in a main deck opening (x = 40 m, y = 16 m).*

Table II. *Temperature range under the ceiling at different time steps. For temperature field see Figure 36.*

Time [s]	Range [K]	Range [°C]
300	332…449	59…176
600	388…474	115…201
900	423…506	150…233
1200	445…523	172…250

Table III. *Temperature range near B-wall at different time steps.*

Time [s]	Range [K] above level +3.00	Range [°C] above level +3.00	T_{max} under level +3.00
600	293…703	20…430	907 K
900	293…688	20…415	940 K
1200	293…728	20…455	964 K

The highest temperature values are found in the flame area. In Figure 38 the temperature field on cross section x = 58 m is shown with a modified scale. The highest temperature values on the plane are about 1380 K below the main deck and 1500 K below the level +3.00 m.

Gas temperature under the main deck is given in Figure 39 on level +12.00 m. Highest values are near 1400 K (about 1100°C) in the plume area. The high temperature area under the deck is not very large, although the smoke spreads also there.

The more detailed incident radiation heat flux on B-wall is given in Figure 40. The maximum incident flux on the main deck level is in the range 24–30 kW/m² at different time steps between 600 s and 1200 s.

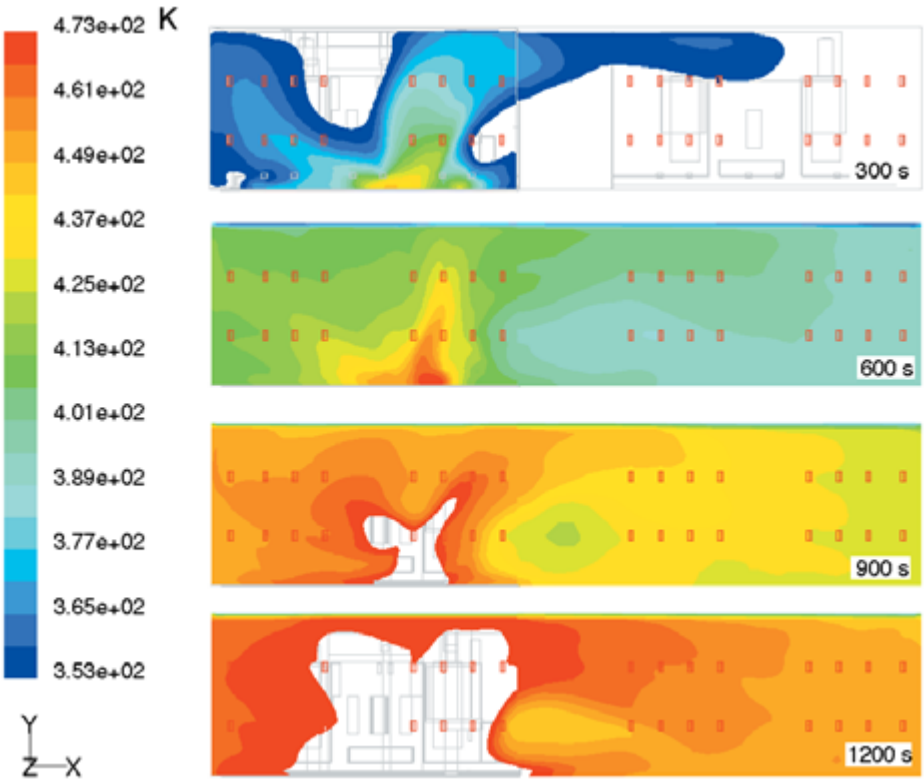

Figure 36. *Temperature field under the ceiling at different time steps. Shown range 353–473 K (80–200°C). The level is +32.00 m, i.e. 0.5 meters below the ceiling surface. The areas without colour denote temperature outside the scale range.*

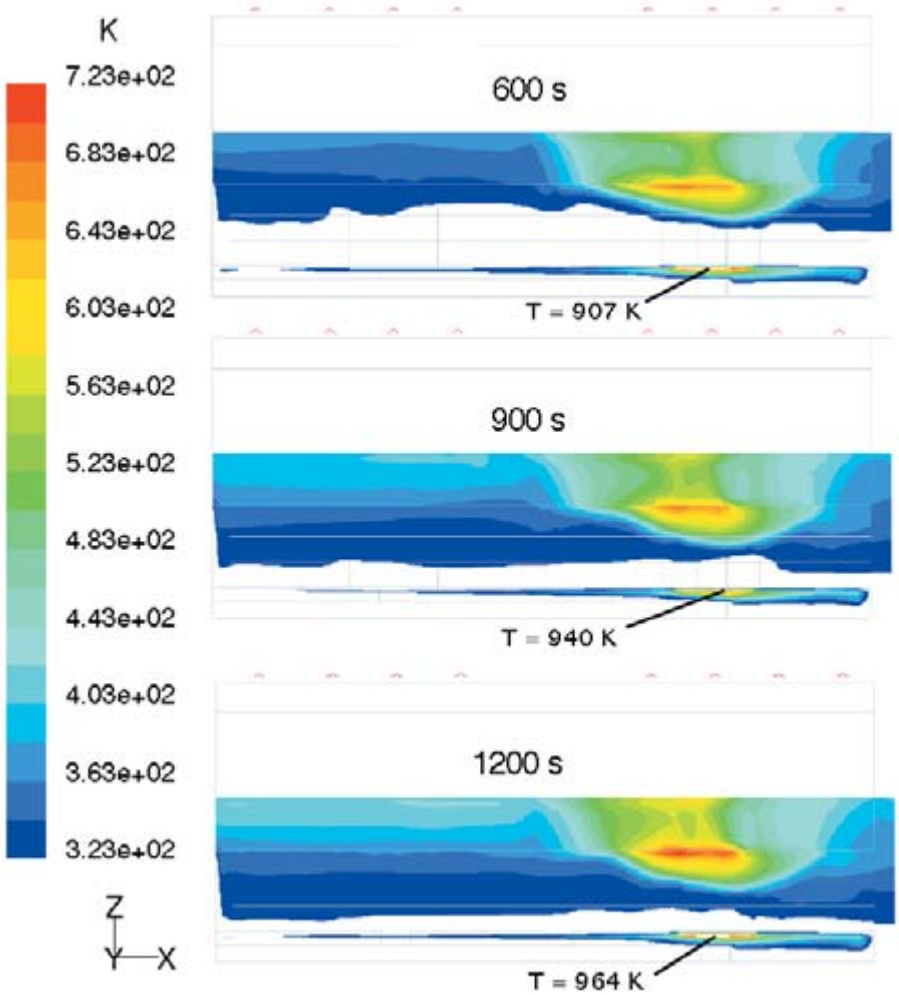

Figure 37. *Temperature range near B-wall at different time steps on unit 1 side. The shown plane is 0.5 m from the wall. Shown range is 323–723 K (50–450°C). The maximum values are found below level +3.00 m. The other local maximum is at the level +12.60 m.*

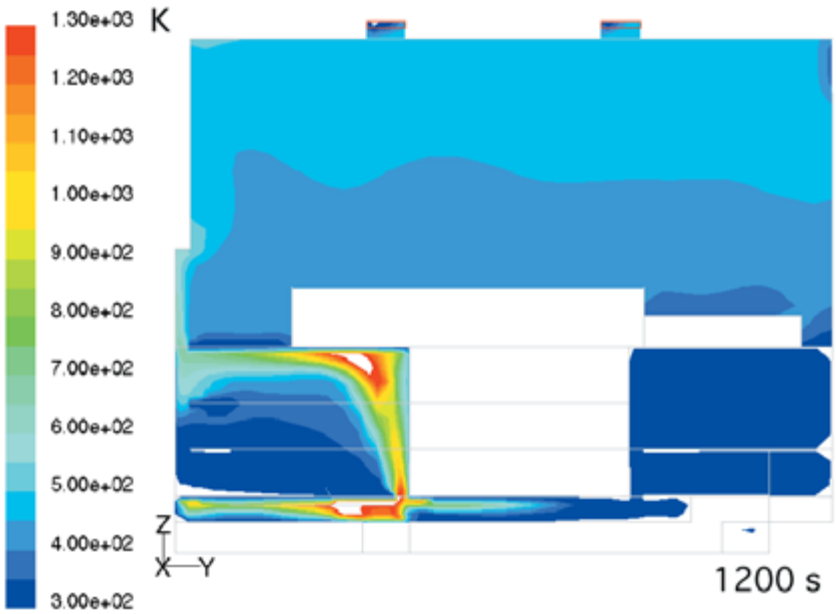

Figure 38. *Temperature field on plane x = 58.75 m at 1200 s.*

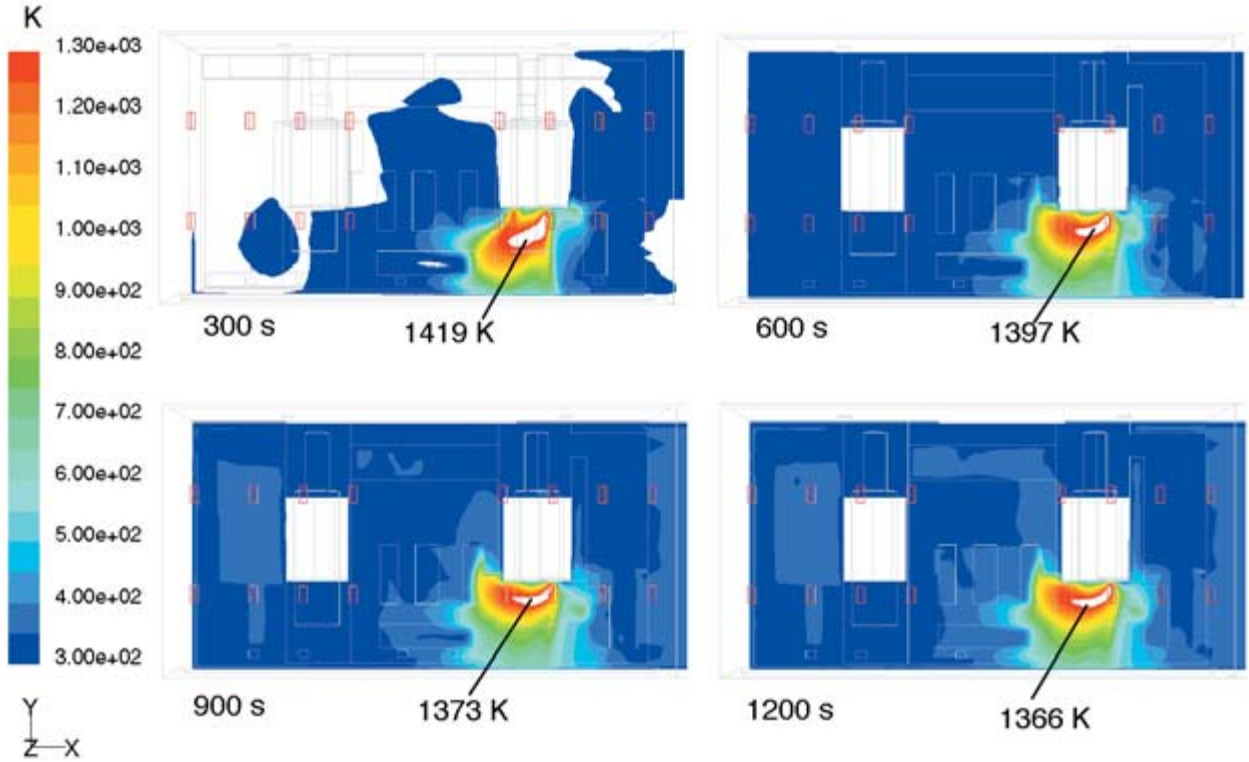

Figure 39. *Gas temperature under the main deck on level +12.00 m.*

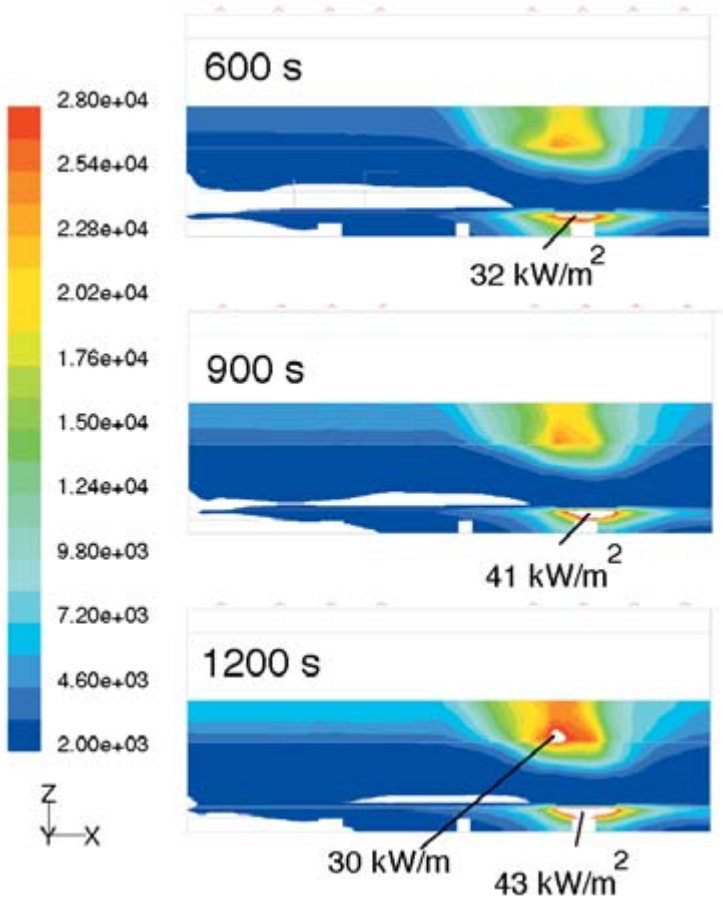

Figure 40. *Incident radiation on B-wall (only unit 1 side) at different time steps. The local maximums at the main deck level are 24 kW/m², 24 kW/m² and 30 kW/m² at time steps 600–1200 s respectively.*

4.7 Amount of oxygen

The amount of oxygen remains sufficient for burning during the whole fire. The building is so large that lack of oxygen influences burning rate only locally where fuel supply is large. Also in these locations in the neighbourhood there exists oxygen to burn the fuel at a later stage. The oxygen mass fraction is given on plane x = 58.75 m in Figure 41.

4.8 Heat load to structures

The general heat load to the tunnels 2 and 4 adjacent to tunnel 3 seems not to be very hard according to this simulation. Ventilation and cool air circulation keeps fresh air on the bottom level. That helps in removing the hot layer from the basement through the openings. That fresh air also cools the tunnel walls.

At B-wall heat load under the basement level +3.00 m is limited essentially to the flame area. The load is very high. The other interesting range is above level +9.00 m up to the level +19.00 m, where the plume hits the wall. The local maximum at the main deck level are 24 kW/m² (600 s), 24 kW/m² (900 s) and 32 kW/m² (1200 s). The consequences of the heat load depend on the structure thickness and the equipment on the other side of the wall. The hall structural metal frame is insulated against fire but the wall itself is bare concrete up to the level +19.00 m. Above this the new wall is insulated up to the ceiling.

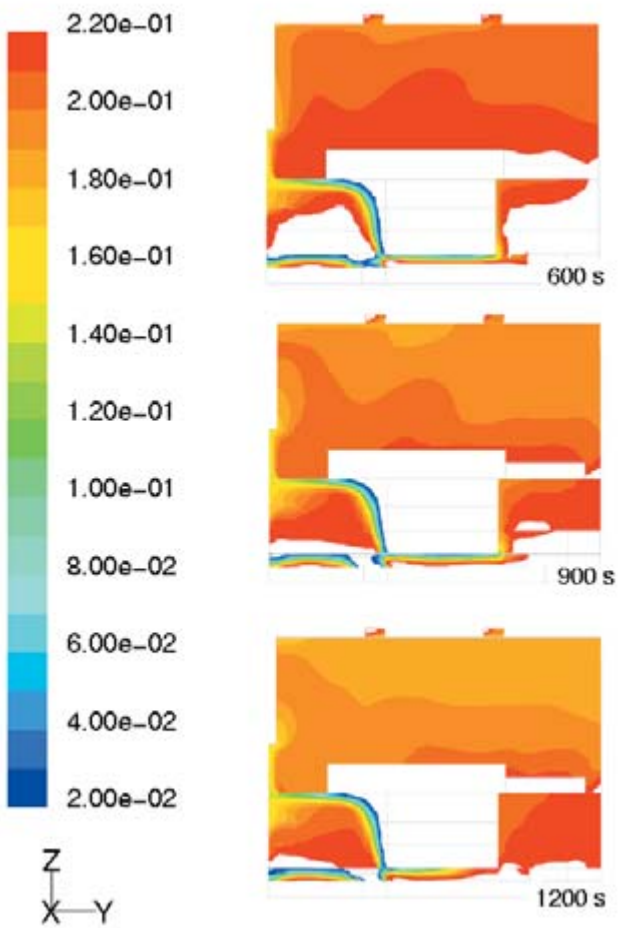

Figure 41. *Oxygen mass fraction on plane x = 58.75 m at different time steps.*

The temperature load to the ceiling is not very heavy according to the simulation. With the applied heat release rate of 150 MW the temperature under the ceiling is about 495 K (220°C) which is not high considering the strength of the steel material. The temperature is still rising after 20 minutes simulation time. The high temperature area is limited to the plume location at least at this simulated time span of 20 minutes. It is not possible to make any justified estimate about the roof integrity without detailed structural analysis.

One interest in the task was to find out if the feed water pumps located between the turbines on level +3.00 m on the unit 2 side are in danger if there is a fire on unit 1 side. According to this simulation, the heat load of those objects does not differ essentially from the normal operating conditions. The fire wall which reaches the main deck +12.60 m on unit 2 side separates the lower part of the unit efficiently and keeps the cool air behind it practically preventing hot gas penetration below the main deck on unit 2 side. In the case there are openings to the lower part of unit 2 from outside (open doors etc.) air leaks take place to the hall direction, because the pressure is lower in the hall than in the free atmosphere due to the hot gases in the hall. That might help keeping the temperature low under the main deck of unit 2.

The local gas temperature, velocity and incident radiation flux to the surfaces is shown in Figures 42–52 in several locations and time steps. In Figure 42 the heat flux to tunnel 2 is rather low at later time steps. The reason for this can be seen from the flow field show in Figure 43 that shows how fresh air flows over tunnel 2 towards the fire source. This keeps the hot layer thinner than it otherwise would be. The heat load to tunnel 4 is higher, especially near the B-wall end where the fire is located.

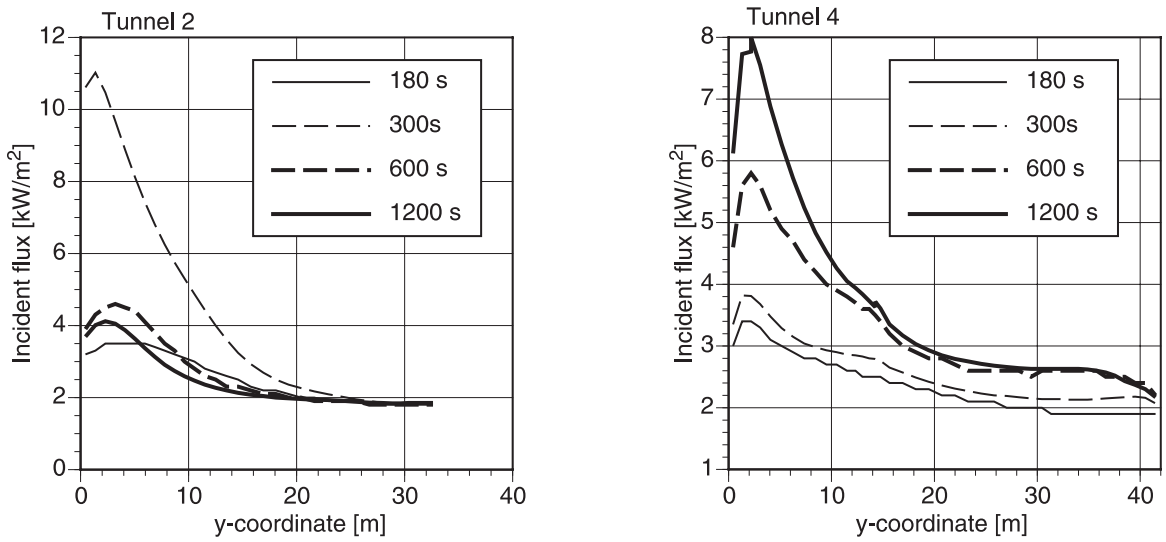

Figure 42. *Distribution of radiation heat flux to cable tunnels 2 and 4. For tunnel 2 the values are taken from the top of the tunnel on level +1.60 m and for tunnel 4 on level +2.60 m.*

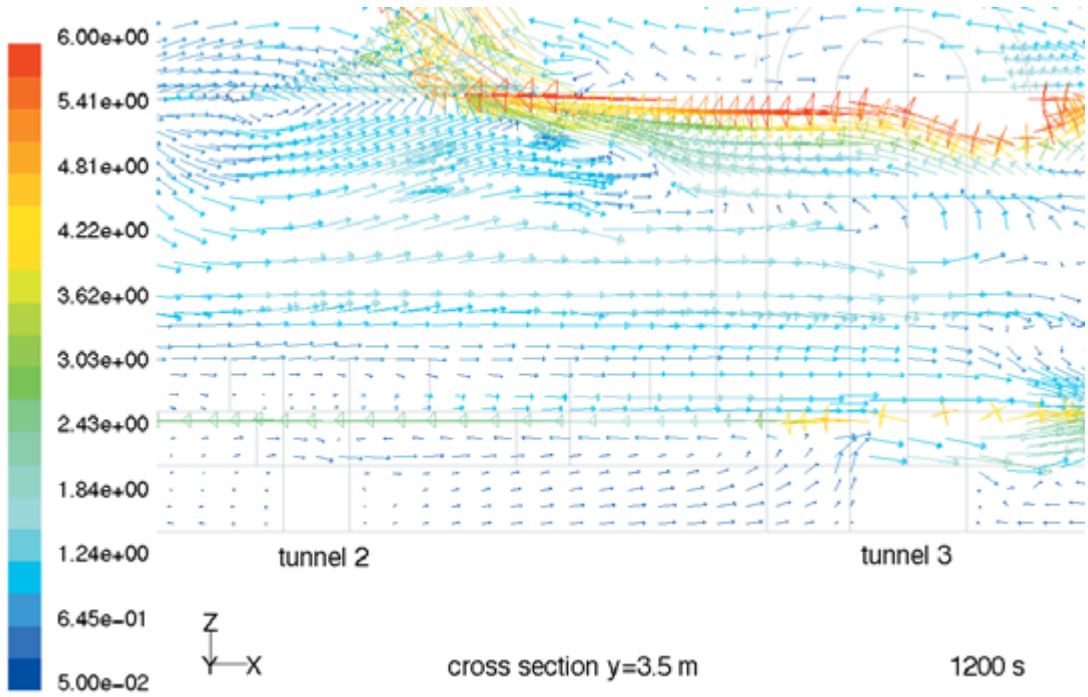

Figure 43. *Detail of flow field on cross section y = 3.5 m at time 1200 s. Velocity scale is in m/s.*

The temperature profiles along tunnels 2 and 4 are given in Figure 44 and flow velocity magnitude in Figure 45. Of these two cable tunnels, tunnel 4 experiences higher thermal load, as both radiation and convective fluxes are higher on that side. The sample points of tunnel 4 are on level +2.60 m when points of tunnel 2 they are on level +1.6 m.

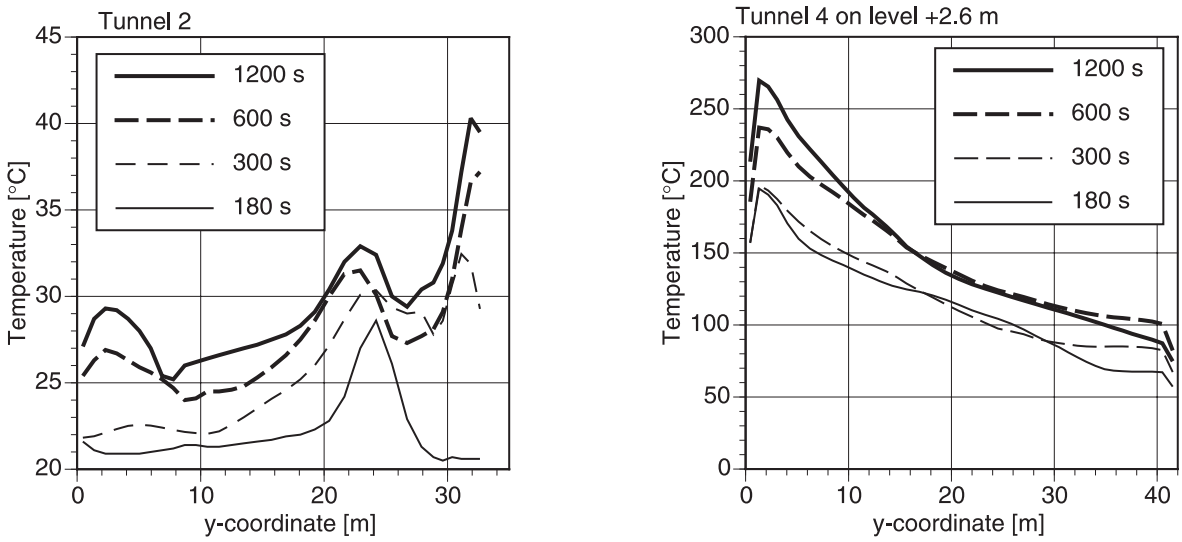

Figure 44. *Temperature profile along cable tunnels 2 (on level +1.60 m) and 4 at different time steps.*

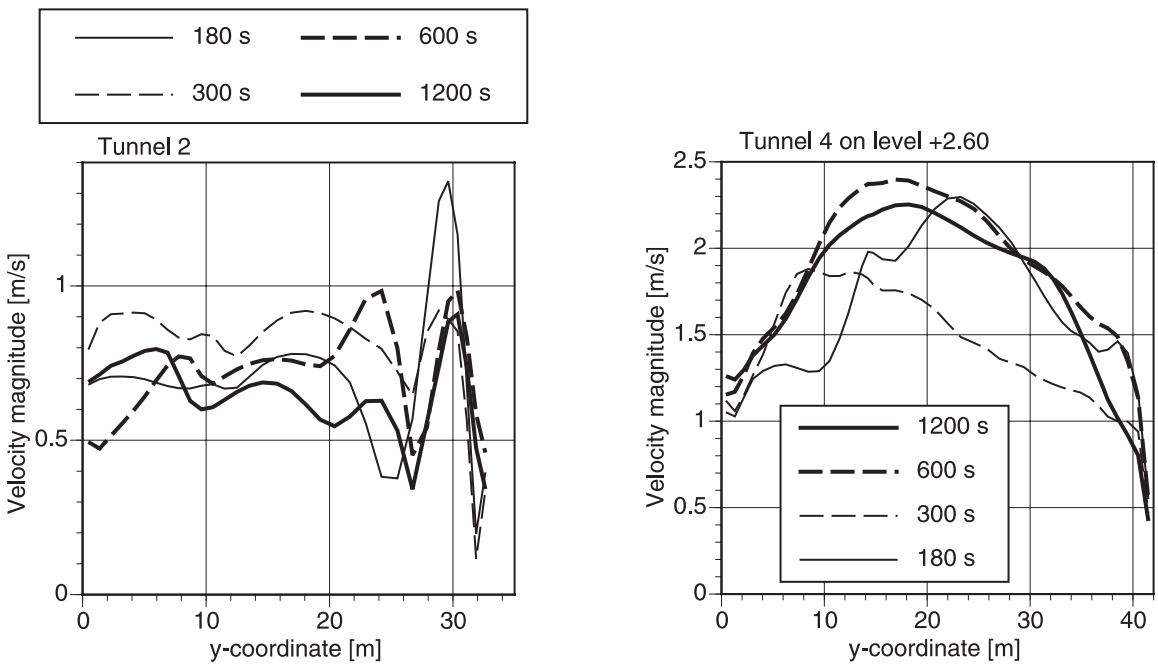

Figure 45. *Velocity magnitude of flow by tunnels 2 and 4 at different time steps.*

Radiation, temperature and velocity on the opposite A-wall below the floor +3.00 m is given in Figure 46 and 47. The velocity peaks in Figure 47 are at the flow inlets. Radiation heat flux on B-wall is shown in Figures 48 and 49.

Gas temperature profiles on B-wall are given in Figure 50. Velocity magnitude by the B-wall is given in Figures 51 and 52.

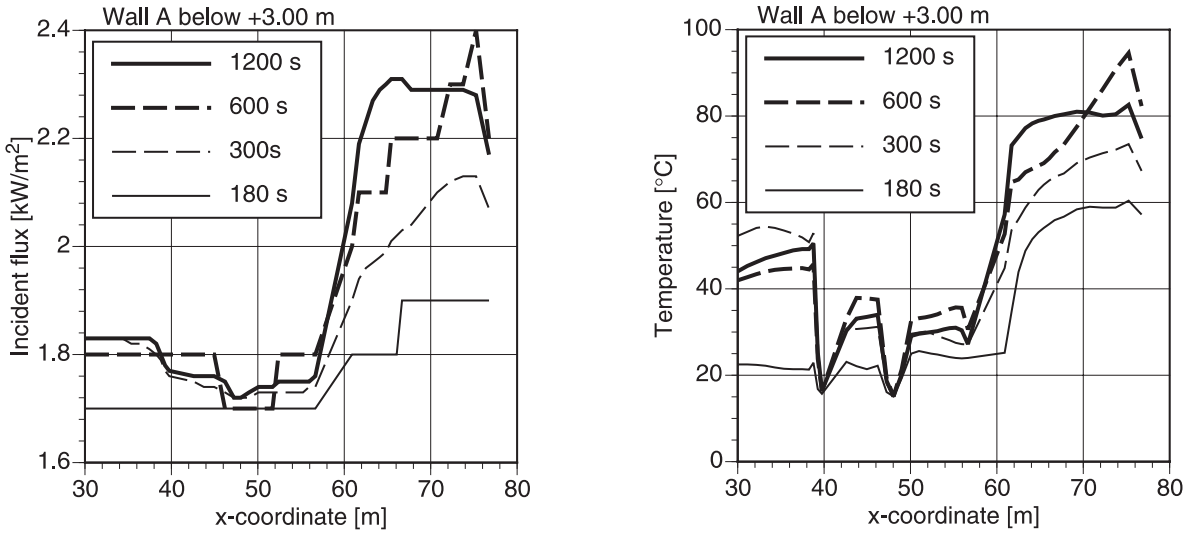

Figure 46. *Incident radiation and local temperature on A-wall at different time steps.*

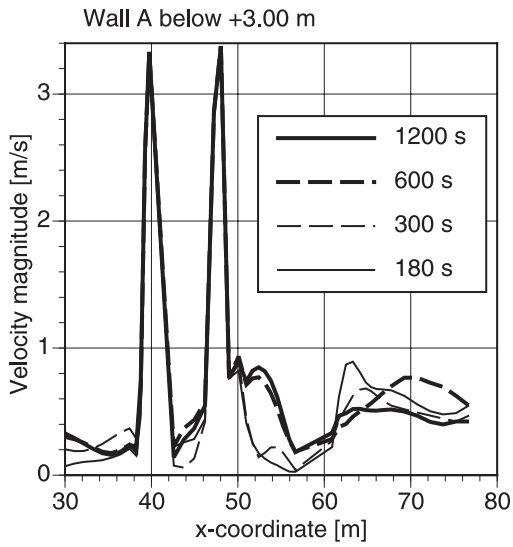

Figure 47. *Flow velocity magnitude on A-wall below the floor +3.00 m.*

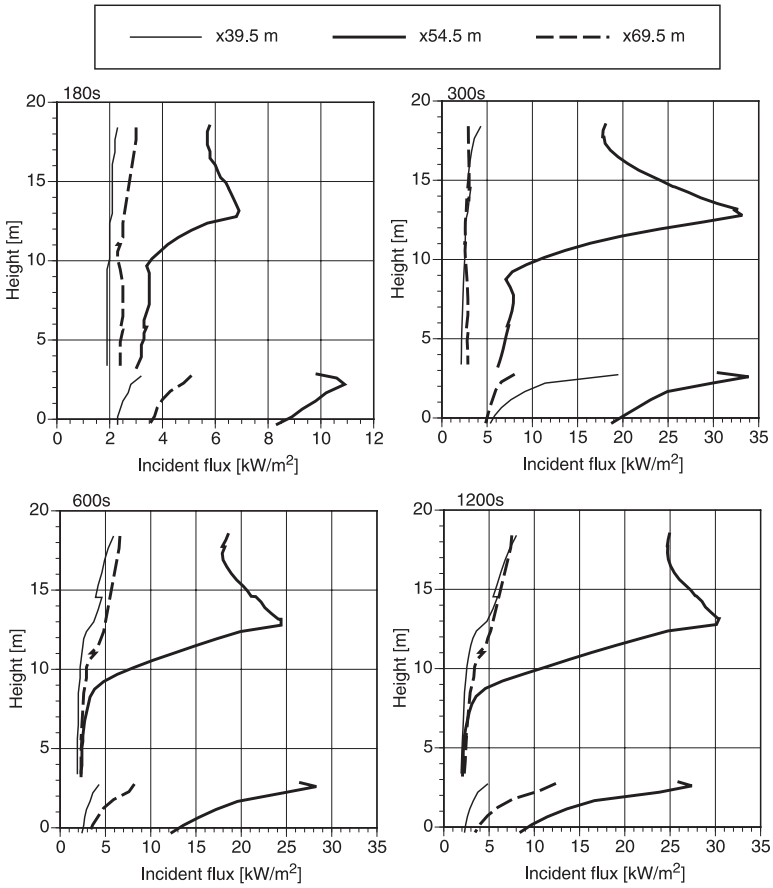

Figure 48. *Incident radiation flux on B-wall at the location of maximum radiation flux and on locations 15 m to both directions.*

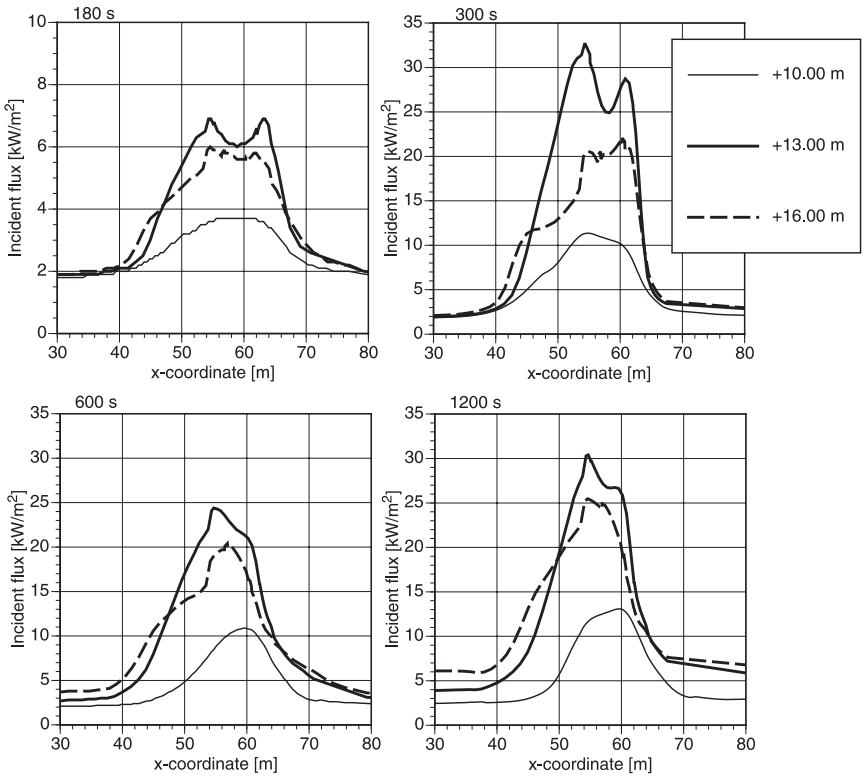

Figure 49. *Incident radiation flux on B-wall at different time steps on levels +10.00 m, +13.00 m and +16.00 m.*

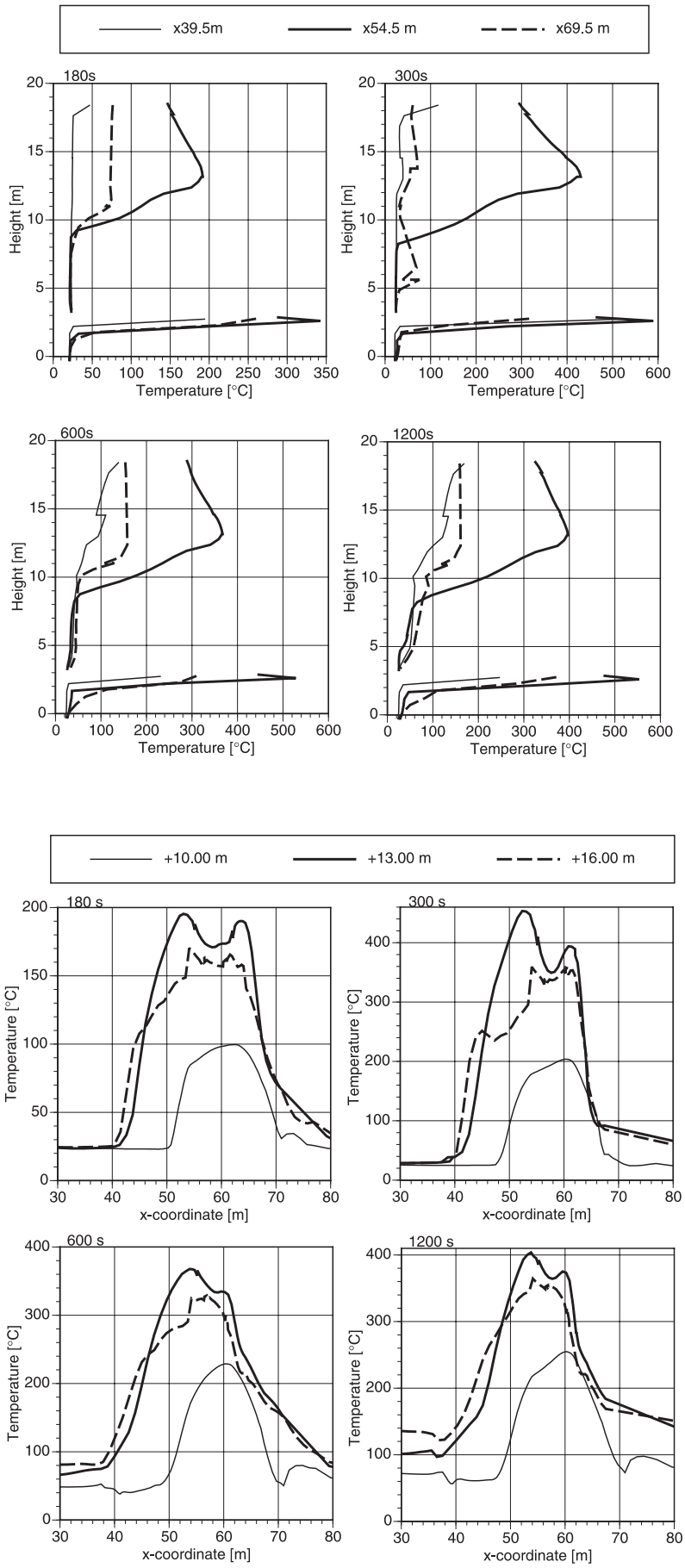

Figure 50. *Vertical and horizontal temperature profiles on B-wall at different time steps.*

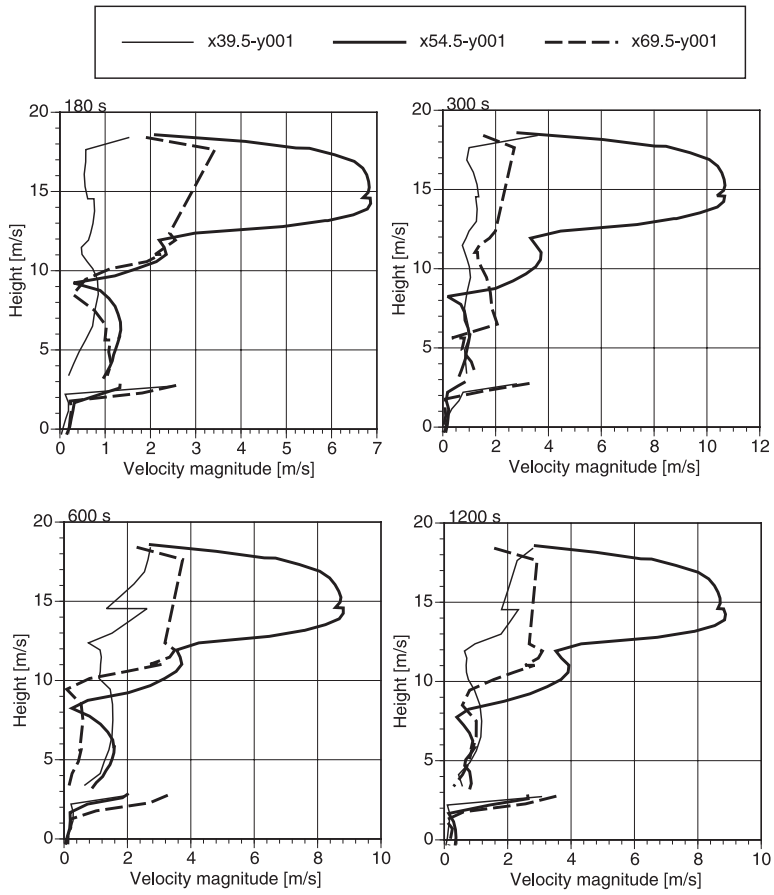

Figure 51. *Velocity magnitude on vertical profiles by B-wall at different time steps.*

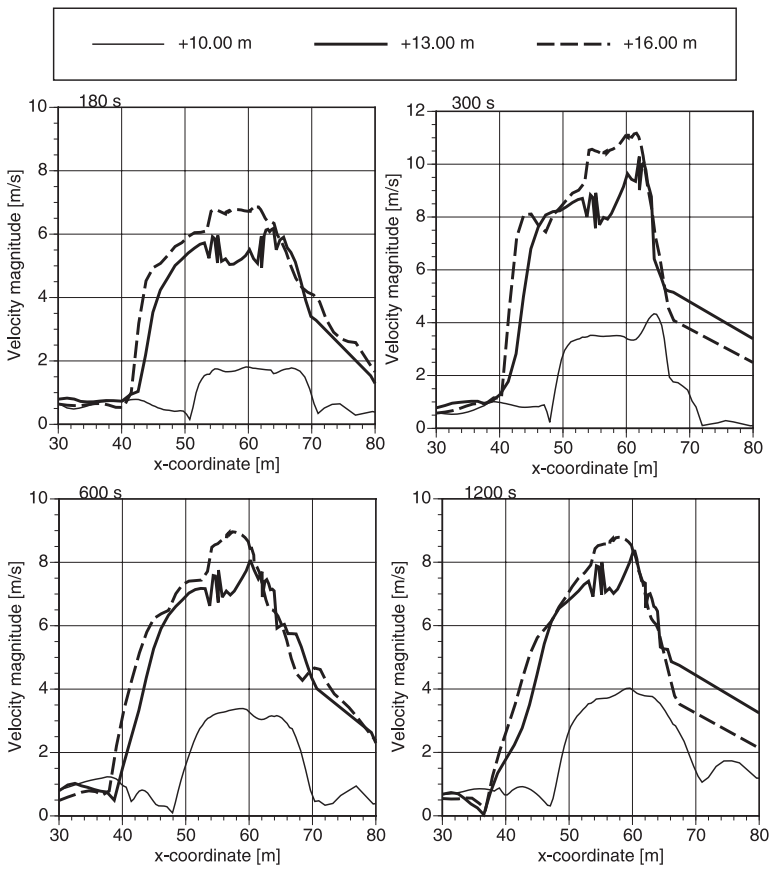

Figure 52. *Velocity magnitude on horizontal profiles by the B-wall at different times steps.*

4.9 Fire with larger heat release rate

An additional scenario, in which the heat release rate is increased from 150 MW to 200 MW after 12 minutes, was simulated starting from the previous results. The heat release rate is the most important single parameter that governs the fire development, which can be seen from the temperature values below the ceiling given in Figure 53. In this case it is probable that the windows on the upper part of the A-wall are broken due to high temperature thus increasing the hall ventilation.

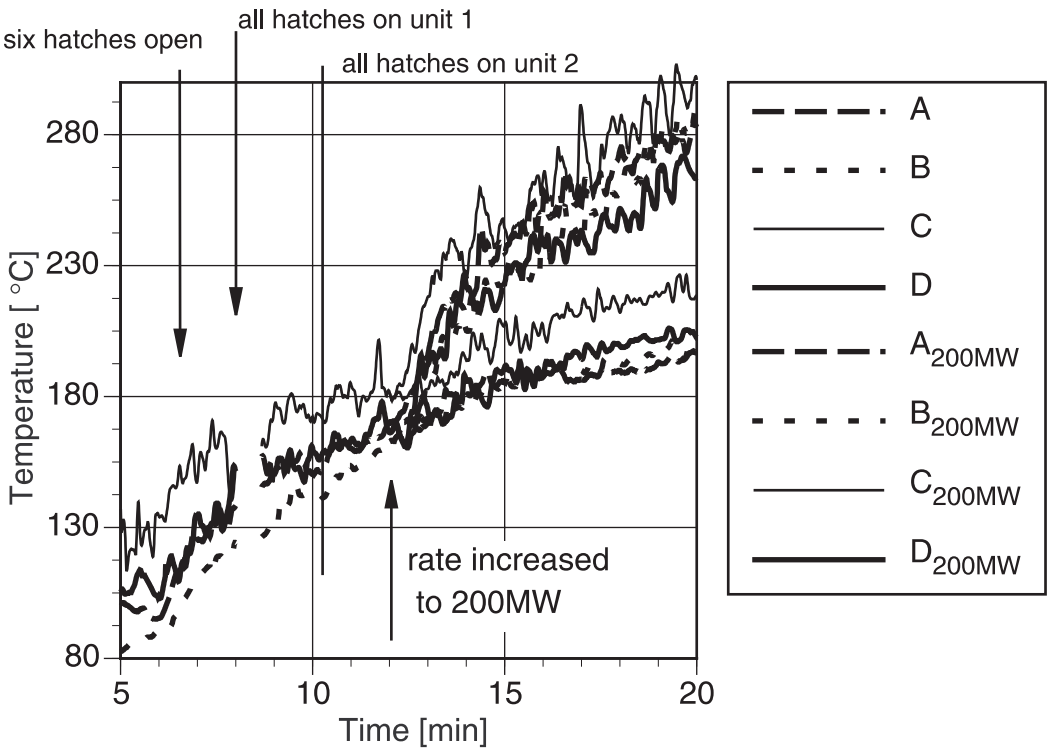

Figure 53. *Temperature values below the smoke hatches A–D in the case of larger heat release rate of 200 MW. The previous lower temperature values with heat release rate of 150 MW are given for comparison.*

5 General estimates about the simulation

In this simulation the main interest has been in the general flow behaviour in the large turbine hall in a case of an oil pool fire. The fuel release rate is given in advance. In the large and rather complex geometry of the hall, the main obstacles and decks that limit fluid flow are taken into account. The turbine hall is common to the two units of the power station. Special attention is paid to the fire source and plume area with main deck openings by refining the grid locally at these locations.

The grid is considered to be good in the areas of main interest. Under the deck +3.00 m the grid is not fine enough to describe the detailed hot layer spread across the whole deck. The estimate of the hot layer has to be considered with care on that area. Although the local accuracy (temperature gradients, local extreme values) may suffer from the grid quality, the general behaviour is expected to be correct.

Oil leak takes place under the turbine 2 on unit 1 where oil is ignited immediately and it flows down from the level of main deck to the lowest level on the side of the heat exchanger. Oil forms a pool on the floor and on one cable tunnel. The applied maximum fuel release rate corresponds to about 150 MW fire rate. The heat load to the adjacent tunnels with redundant cable routes and to the sidewall of the turbine hall is calculated. Behind the uninsulated sidewall there exists electronic device that may be damaged due to the heat load. The evaluation of possible damage must be done separately using the estimated heat load given here and is not part of this work. The location of the oil pool has been chosen with reasoning to a realistic place. However, the fire may locate also in some other place. In that case the similar heat load is exposed to a new area.

In the simulation it is assumed that the ventilation operates at nominal rate. Under these conditions the heat load to the adjacent tunnels seems not to be very high. The maximum incident radiation flux is about 5 kW/m^2 and gas temperature above the cable tunnels is 250–300°C. However, this case has to be examined more thoroughly using detailed information of the tunnel structure. The sidewall is effected by more severe heat load. The maximum radiation flux is 32–43 kW/m^2 under the level +3.00 m and 24–30 kW/m^2 near the main deck at times 10–20 minutes from ignition. The maximum gas temperature is 630–690°C under the level +3.00 m and 430–450°C near the main deck during the same time interval. Heating up of the cable tunnel 3 and the adjacent electrical rooms and the effects of elevated temperature to plant safety are out of the scope of this study. They will be studied separately, e.g., using the calculated heat loads from this simulation as initial data.

It might have been advantageous to refine the grid locally above the main deck in the plume region. With the present grid it is possible that the plume mixing is too high giving too low local temperature values in places where the plume hits the ceiling. The general hot layer temperature is considered to be right. The temperature under the ceiling reaches in rather large area the level of 200–250°C within 20 minutes in the case where the smoke hatches are open and remove part of the heat. This temperature alone is not considered too high to affect the material strength. The stability of the truss structure supporting the roof should be checked using more detailed information of the structure. After 20 minutes the temperature under the ceiling is still rising.

For the heat transfer boundary conditions, constant temperature on concrete walls is assumed. In practice, the wall surface temperature rises during the fire thus reducing the net radiation flux to the surface. Due to the high number of cells it was not possible to increase the computational effort by calculating the detailed heat transfer inside the massive walls. The given radiation parameter is the incident (incoming) radiation flux which does not include any assumption of the boundary condition. This can be used with confident as the boundary condition for more detailed heat transfer estimates together with the local gas temperature values.

It is assumed that the windows on the upper edge of A-wall are not broken. During the 20 minute simulation time, temperature just reaches 200°C by the windows. The window area is about 3 meters in height. About one third of that can be opened by remote control. If the windows are opened or broken, the ventilation may be enhanced depending on the wind conditions. Considering the temperature field, the closed windows case is a conservative assumption.

References

1. Huhtanen Risto. Numerical fire modeling of a turbine hall. 2nd International Symposium for Fire Safety Science. Tokyo, 13–17 June 1988. Hemisphere Publishing Corp. (1989), pp. 771–779.